BMC Physiology

BioMed Central

Research article

Open Access

Physiological responses of *Daphnia pulex* to acid stress

Anna K Weber and Ralph Pirow*

Address: Institute of Zoophysiology, University of Münster, Münster, Germany

Email: Anna K Weber - akweber@gmx.de; Ralph Pirow* - pirow@uni-muenster.de

* Corresponding author

Published: 21 April 2009

BMC Physiology 2009, **9**:9 doi:10.1186/1472-6793-9-9

Received: 29 February 2008

Accepted: 21 April 2009

This article is available from: http://www.biomedcentral.com/1472-6793/9/9

Abstract

Background: Acidity exerts a determining influence on the composition and diversity of freshwater faunas. While the physiological implications of freshwater acidification have been intensively studied in teleost fish and crayfish, much less is known about the acid-stress physiology of ecologically important groups such as cladoceran zooplankton. This study analyzed the extracellular acid-base state and CO_2 partial pressure (P_{CO2}), circulation and ventilation, as well as the respiration rate of *Daphnia pulex* acclimated to acidic (pH 5.5 and 6.0) and circumneutral (pH 7.8) conditions.

Results: *D. pulex* had a remarkably high extracellular pH of 8.33 and extracellular P_{CO2} of 0.56 kPa under normal ambient conditions (pH 7.8 and normocapnia). The hemolymph had a high bicarbonate concentration of 20.9 mM and a total buffer value of 51.5 meq L^{-1} pH^{-1}. Bicarbonate covered 93% of the total buffer value. Acidic conditions induced a slight acidosis (ΔpH = 0.16–0.23), a 30–65% bicarbonate loss, and elevated systemic activities (tachycardia, hyperventilation, hypermetabolism). pH 6.0 animals partly compensated the bicarbonate loss by increasing the non-bicarbonate buffer value from 2.0 to 5.1 meq L^{-1} pH^{-1}. The extracellular P_{CO2} of pH 5.5 animals was significantly reduced to 0.33 kPa, and these animals showed the highest tolerance to a short-term exposure to severe acid stress.

Conclusion: Chronic exposure to acidic conditions had a pervasive impact on *Daphnia*'s physiology including acid-base balance, extracellular P_{CO2}, circulation and ventilation, and energy metabolism. Compensatory changes in extracellular non-bicarbonate buffering capacity and the improved tolerance to severe acid stress indicated the activation of defense mechanisms which may result from gene-expression mediated adjustments in hemolymph buffer proteins and in epithelial properties. Mechanistic analyses of the interdependence between extracellular acid-base balance and CO_2 transport raised the question of whether a carbonic anhydrase (CA) is involved in the catalysis of the CO_2-HCO_3^--H^+ reaction, which led to the discovery of 31 CA-genes in the genome of *D. pulex*.

Background

Freshwater acidification is an important stressor that affects the structure of zooplankton communities in lake ecosystems. Acidification may arise from natural processes such as spring acid episodes [1,2], acid rock drainage [3] and volcanism [4,5], or from anthropogenic activities including fossil fuels burning [6,7], agriculture measures [8], dredging of waterways [9,10] and mining-related processes (e.g. acid mine drainage, recultivation and flooding of former mining pits) [11,12]. pH levels below 5–6 generally decrease the zooplankton species richness compared to circumneutral pH conditions [13-16]. Among the zooplankton, crustaceans of the genus *Daphnia* are usually less abundant in acidified lakes while other (non-daphnid) cladocerans, calanoid copepods, and insects (e.g. *Chaoborus* larvae and corixids) may increase in importance or even become dominating [15,17]. The mechanisms behind these changes in the zooplankton community structure are manifold. They include a differential physiological sensitivity to acid stress [14,18,19], a differential tolerance against toxic metal species [20-22], which become more soluble under acidic conditions, as well as altered biotic interactions arising from the effect of pH on phytoplankton and planktivore communities [14,23].

It is well-known that the physiological sensitivity of aquatic animals to acidic conditions is associated with iono- and osmoregulatory processes [24,25]. Faced with the continuous diffusive gain of water and loss of ions, freshwater animals generally have to minimize their whole-body permeability to water and/or ions and additionally require compensatory uptake mechanisms for sodium and chloride to maintain a steady-state ion balance [26]. While data on whole-body water permeability of freshwater zooplankton are essentially lacking [27-29], there is some information on sodium permeability. In general, acid-tolerant species such as aquatic insects have a relatively low sodium permeability in comparison to cladocerans [18,30-32]. In the acid-sensitive daphnids, the inability to survive long term below pH 5 is correlated with the net loss of body sodium due to an accelerated rate of Na^+ loss and a reduced rate of Na^+ uptake [33,34], a process that is additionally influenced by the ambient calcium concentration [35].

The acidification-induced impairment of sodium uptake in daphnids suggests that the transport of sodium across the epipodites – the *so-called* 'branchial sacs' [36] – is linked with proton extrusion [33,35], as it is in the gills of other freshwater animals such as fish and crayfish [37-40]. The protons arise from the catalyzed hydration of CO_2 by a cytoplasmic carbonic anhydrase in the ionoregulatory epithelia. This reaction produces HCO_3^- which is then excreted in exchange for chloride [41]. The interdependence between ionoregulatory processes, acid-base balance, and CO_2 transport explains the strong impact of acid stress on the physiology of many freshwater animals. However, in contrast to the detailed information on teleost fish [24] and crayfish [25], the physiological implications of acid stress in daphnids have remained largely unexplored. Daphnids are important model organisms in ecotoxicology, and there is a growing interest in establishing mechanistic links between molecular stress responses and organismal stress responses [42-47]. Understanding the specific physiology of *Daphnia* may help to elucidate the modes of action of environmental toxicants [48,49].

The present study provides the experimental, methodical, and conceptual framework to analyze the acid-stress physiology of daphnids. Preliminary tests with *Daphnia pulex* yielded the appropriate acclimation conditions which guaranteed the survival, growth, and reproduction under acidic (pH 5.5 and 6.0) and circumneutral conditions (pH 7.8). Based on these stable laboratory populations, we determined the buffer characteristics from microliter hemolymph samples, analyzed the extracellular acid-base state by microspectralfluorometry using the pH-sensitive dye cSNARF-1, and studied the responses to a short-term exposure to severe acid stress (pH 3–4). Circulation, ventilation and respiration were additionally analyzed and served as diagnostic indicators for the interpretation of acid-base disturbances. Moreover, reproduction was monitored to assess acidification-induced changes in maintenance costs and energy-and-mass budget. Finally, the implications of the presence or absence of an extracellular carbonic anhydrase for acid-base balance and circulatory CO_2 transport are discussed.

Results and discussion

Acid-base balance under normal conditions

A rather alkaline extracellular pH of 8.334 ± 0.006 (mean ± S.E., N = 4) was measured in the heart region of animals which were raised and examined under normal conditions (i.e. ambient pH = 7.8, P_{CO2} = 0.035 kPa, and 20°C). By taking the characteristics and the variability of the hemolymph buffer curves (Table 1) into account, the mean *in vivo* pH corresponded to an equilibrium P_{CO2} of 0.56 ± 0.02 kPa (means ± S.E., N = 3 buffer curves) and a hemolymph bicarbonate concentration of 20.9 ± 0.7 mM (Table 2 and Figure 1A, open triangle). The derived P_{CO2} value is a representative measure of the extracellular P_{CO2} in the heart reagion as long as the $CO_2+H_2O \leftrightarrow H^+ + HCO_3^-$ reaction in the hemolymph can reasonably be assumed to be in equilibrium. The information on the hemolymph

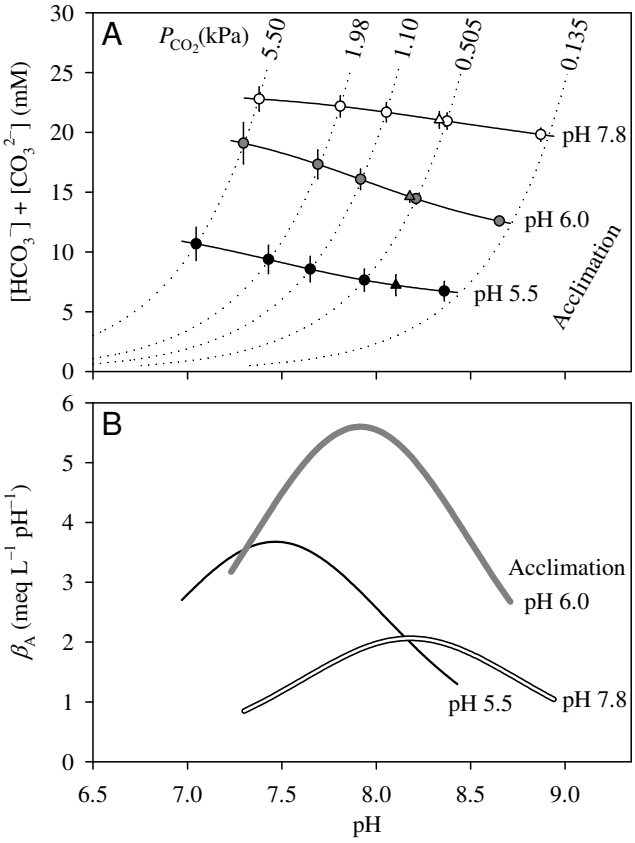

Figure 1
Hemolymph buffer curves and non-bicarbonate buffer values. (A) Hemolymph buffer curves of animals raised at 20°C at pH 7.8 (open symbols), pH 6.0 (grey-filled symbols), and pH 5.5 (filled symbols). The symbols represent the mean of a three-fold determination. The error in the concentration of chemically bound CO_2 arises from the standard error in the calculation of CO_2 partial pressure (P_{CO2}) for a given pH (Table 1). The solid lines were calculated using the equations 1–3 and the means of the individual (curve-specific) parameter values given in Table 1. Dotted lines represent the P_{CO2} isobars. The triangles indicate the *in vivo* acid-base state of the respective acclimation groups. (B) Non-bicarbonate buffer values (β_A) calculated from equation 4.

Table 1: Analysis of hemolymph buffer curves and determination of P_{CO2} from pH.

Group	SID (meq L^{-1})	C_A (mM)	pK'_A	rmse
pH 7.8 acclimation	21.1 ± 0.2	2.3 ± 0.3	8.18 ± 0.11	0.003
	24.9 ± 0.3	5.2 ± 0.3		
	23.9 ± 0.2	3.2 ± 0.3		
pH 6.0 acclimation	20.9 ± 0.8	10.4 ± 0.9	7.92 ± 0.11	0.011
	25.0 ± 1.2	14.4 ± 1.1		
	17.1 ± 0.5	4.4 ± 0.7		
pH 5.5 acclimation	13.6 ± 0.4	7.4 ± 0.4	7.46 ± 0.06	0.006
	9.2 ± 0.2	4.4 ± 0.2		
	14.6 ± 0.4	7.4 ± 0.4		

Buffer curves were obtained by measuring the pH of hemolymph samples in dependence on CO_2 partial pressure (P_{CO2}). The three buffer curves of each acclimation group were simultaneously fitted by the binary buffer model (equation 1), using pK'_A as a shared parameter. This means that the value of this parameter was forced to be the same for all three buffer curves. Given are the best-fit parameter values (mean ± standard error) for the strong ion difference (SID), the concentration (C_A) and pK'_A value of the non-bicarbonate buffer, and the the standard error of the fit (rmse, root mean squared error). The number for the degrees of freedom (i.e. the number of data points minus the number of fitted parameters) was 8. The reverse determination of P_{CO2} from pH is exemplified as follows. Given the *in vivo* pH of 8.334, the three calibration buffer curves of the pH 7.8 acclimation group yielded P_{CO2} values of 0.519 ± 0.005 kPa, 0.573 ± 0.006 kPa, and 0.575 ± 0.005 kPa. These individual means were finally averaged to yield an overall mean of 0.556 kPa with a standard error of 0.018 kPa. This standard error therefore reflects the variability among the buffer curves.

buffer curves and the extracellular pH was used to assess the capacity of the extracellular compartment to buffer hydrogen ions of metabolic origin. The hemolymph had a total buffer value (β_T) of 51.5 meq L^{-1} pH^{-1} (Table 2). Bicarbonate covered 93% of β_T, and the non-bicarbonate buffer value (β_A) was 2.0 meq L^{-1} pH^{-1}.

Given the extracellular pH of 8.334, which is markedly higher than the circumneutral values of other water-breathing crustaceans (Table 3) [50-70], one is tempted to assume that *Daphnia pulex* is in a state of permanent respiratory alkalosis. Indeed, the filter-feeding mode of life of daphnids is inevitably associated with high ventilation rates (e.g. 0.75 mm^3 s^{-1} [mm^{-3} body volume] for *D. magna*) [71], which should favor the wash-out of carbon dioxide from the hemolymph. However, the present study gave no indication for a respiratory hypocapnia in *D. pulex*, since the extracellular pH suggested an equilibrium P_{CO2} of 0.56 kPa, which is higher than the typical P_{CO2} values (0.2–0.5 kPa, Table 3) in the prebranchial and postbranchial hemolymph of other water-breathing crustaceans. If the equilibrium P_{CO2} in the postbranchial hemolymph of *D. pulex* would approach the low value of, say, 0.2 kPa, an extreme alkalosis (pH 8.75) would occur. Taking the scaling relationship between metabolic rate and body size into account [72], the exceptional acid-base state of these small crustaceans seems to be determined by two main factors: (i) a high, specific metabolic rate, which contributes to the elevated P_{CO2} levels, and (ii) a high bicarbonate buffer value, which might be a pre-adaptive feature to cope with a highly variable, physiologically challenging environment.

One may argue that the *in vivo* results are to some extent influenced by the experimental procedures, which

Table 2: Comparison of acid-base, systemic and respiratory variables among the different acclimation groups.

Physiological Variable	pH 7.8 acclimation	pH 6.0 acclimation	pH 5.5 acclimation	Significant difference among acclimation groups
pH	8.334 ± 0.006†	8.177 ± 0.025	8.104 ± 0.008#	***
P_{CO_2} (kPa)	0.56 ± 0.02	0.56 ± 0.02	0.33 ± 0.04#	***
HCO_3^- (mM)	20.9 ± 0.7	14.6 ± 0.5#	7.2 ± 0.9#	***
CO_3^{2-} (mM)	0.153 ± 0.005	0.074 ± 0.003	0.031 ± 0.007	***
β_A (meq L^{-1} pH^{-1})	2.0	5.1	2.2	not tested
β_B (meq L^{-1} pH^{-1})	48.1	33.5	16.6	not tested
β_C (meq L^{-1} pH^{-1})	0.70	0.34	0.14	not tested
β_T (meq L^{-1} pH^{-1})	51.5	39.4	19.1	not tested
f_H (min^{-1})	205 ± 10†	246 ± 18	299 ± 12#	**
f_A (min^{-1})	374 ± 32†	427 ± 58	500 ± 6#	*
$\dot{M}_{O_2}$ (nmol h^{-1} mm^{-3})	1.53 ± 0.09	1.95 ± 0.07†#	1.41 ± 0.14†	**

P_{CO2}, CO_2 partial pressure; β_A, buffer value of the non-bicarbonate buffer; β_B and β_C, bicarbonate and carbonate buffer value; β_T, total buffer value (= $\beta_A + \beta_B + 2\beta_C$); f_H, heart rate; f_A, appendage beating rate; $\dot{M}_{O_2}$, specific oxygen consumption rate (per cubic body length). Data are expressed as means ± standard error, except for the buffer values which are given as means. The number of independent determinations (*N*) is 3, if not otherwise indicated. The P_{CO2} was calculated from the mean pH value and the three corresponding buffer curves (Table 1). Asterisks indicate significant differences among the acclimation groups (*$P < 0.05$, **$P < 0.01$, ***$P < 0.001$). #significant difference between an acid-stress (pH 6.0 or pH 5.5) group and the control (pH 7.8) group. †$N = 4$.

required the microinjection of a pH-sensitive dye into the circulatory system of immobilized animals. Previous studies [71,73-75] have shown that the immobilization does not induce any noticable physiological disturbances, provided that the animals have the chance to acclimate to the experimental conditions for at least 30 min. Immobilized animals of *D. magna*, for example, exhibit the typical resting values in heart rate (f_H) and appendage beating rate (f_A) and respond in a predictable manner to changes in abiotic [73-75] and biotic factors [71]. The microinjection procecure, however, is known to induce a bradycardia in *D. magna* [76] and it did so in *D. pulex*. Our microinjected control animals (pH 7.8 acclimation) had a f_H of 205 ± 10 min^{-1} ($N = 4$), which was significantly lower than that of non-injected animals (310 ± 28 min^{-1}, $N = 5$; *t*-test: $P = 0.01$). In contrast, there was no significant effect on f_A (injected: 374 ± 32 min^{-1}, non-injected: 352 ± 51 min^{-1}; $P = 0.8$). The slower f_H was very likely caused by the increase in hemolymph viscosity due to the injection of the dye-coupled 70-kDa dextrans. Given the 34% reduction in f_H, one may suppose a pertubation in the hemolymph partial pressures of respiratory gases including the P_{CO2}. Theoretical analyses in terms of the CO_2 transport model, which is described below, revealed that the mean extracellular P_{CO2} would be 8% smaller in the absence of a bradycardia. An effect of this magnitude does not invalidate the findings about the exceptional acid-base state of *D. pulex*.

Physiological and visible effects of chronic exposure to acidic conditions

Animals raised and tested under acidic conditions (ambient pH 6.0 and pH 5.5) had extracellular pH values of 8.177 ± 0.025 and 8.104 ± 0.008 ($N = 3$ each), respectively. These values were 0.16–0.23 pH units lower than that of the control (pH 7.8 acclimated) animals. The differences in extracellular pH among the acclimation groups were statistically significant (Table 2). The extracellular P_{CO2} (0.56 ± 0.02 kPa) of the pH 6.0 acclimated animals

Table 3: Acid-base status in Crustacea.

Group/Species	pH	$[HCO_3^-]$ (mM)	P_{CO_2} (kPa)	arterial/ venous	β_A (mM pH^{-1})	*T* (°C)	Medium	Mode of Life	Reference
Branchiopoda									
Daphnia pulex	8.33	21.0	0.56		1.75	20	FW	A	§
Daphnia magna	8.44	13.4	0.28		0.5	20	FW	A	$
Triops cancriformis	7.52	7.6	1.36		2.1	20	FW	A	$
Decapoda									
Astacus astacus	7.78	5.2	0.27	a	6.3	15	FW	A	[79]
Astacus leptodactylus	7.87	4.5	0.26	v	11.6	13	FW	A	[61]
Pacifastacus leniusculus	7.95	8.8#	0.37	a	11.6	15	FW	A	[69]
Austropotamobius pallipes	7.90	6.9#	0.40	a	13.5	15	FW	A	[64]
Orconectes rusticus	7.87	5.8#	0.45	a		15	FW	A	[70]
Orconectes propinquus	7.75	7.0	0.37	a	8	10	FW	A	[78]
Procambarus clarki	7.93	9.9	0.49	a		15	FW	A	[77]
Procambarus clarki	8.17	17.8	0.44	a		15	FW	A	[77]
Procambarus clarki	7.75	7.0	0.40	a			FW	A	[25]
Homarus vulgaris	7.80	5.6	0.26	a	8	15	SW	A	[57]
Homarus gammarus	7.78	9.3	0.44	a	15	15	SW	A	[65]
Palaemon elegans	7.89	5.4#	0.17	a	16	15	SW	A	[59]
Palaemon adspersus	7.85	4–7	0.25	a	4–9	15	SW	A	[68]
Penaeus japonicus	7.58	6.0	0.44	a		18	SW	A	[52]
Carcinus maenas	7.82	3.9	0.15	v	13.3	15	SW	X	[66]
Callinectes sapidus	7.96	8.8	0.40	v	5	22	FW	A	[50]
Scylla serrata	7.68	7.5#	0.48	a	13.2	25	SW	A	[67]
Necora puber	7.90	6.6	0.19	v		15	SW	A	[62]
Cancer magister	7.73	4.5	0.25	a		17	SW	A	[56]
Cancer productus	7.89	9.0	0.30	a		10	SW	A	[53]
Gecarcinus lateralis	7.37	5.9	0.86	a		25	SW	T	[63]
Cardisoma carnifex	7.64	10.3#	0.93	a		28	SW	T	[51]

Table 3: Acid-base status in Crustacea. *(Continued)*

Cyclograpsus lavauxi	7.92	10.9	0.31	a		10	SW	X	[55]
Leptograpsus variegatus	7.90	5.4#	0.24	a		20	SW	X	[58]
Holthusiana transversa	7.33	9.5	0.80	a		25	FW	X	[54]
Amphipoda									
Gammarus pulex	8.00	12.4	0.40	a	2.6	12	FW	A	[60]
Gammarus fossarum	8.00	10.4	0.33	a	3.0	12	FW	A	[60]

Hemolymph acid-base status of various crustaceans in freshwater (FW) and seawater (SW) under aerated conditions at temperature *T*. Postbranchial (a = 'arterial') hemolymph was drawn from the pericardial sinus, whereas prebranchial (v = 'venous') samples were taken from the infrabranchial sinus at the base of the walking leg. For each species, the typical mode of life (A = aquatic, T = terrestrial, X = amphibious) is indicated. #total CO_2, §this study, $unpublished data.

was virtually the same as that of the control group. In contrast, pH 5.5 animals had a significantly lower extracellular P_{CO2} of 0.33 ± 0.04 kPa (Table 2).

The slight acidosis in the extracellular fluid was associated with a significant (30–65%) reduction in hemolymph bicarbonate concentration to 14.6 ± 0.5 mM in pH 6.0 animals and 7.2 ± 0.9 mM in pH 5.5 animals (Table 2 and Figure 1A, gray and black triangles). Reductions of similar relative magnitude have been observed in freshwater crayfish [77-79]. This depletion in hemolymph bicarbonate, by the entry of acidic equivalents from the ambient medium (see below), caused a proportional reduction in the bicarbonate buffer value (β_B). The pH 6.0 animals partly compensated the 30% reduction in β_B by increasing the non-bicarbonate buffer value (β_A) from 2.0 to 5.1 meq L^{-1} pH^{-1}, while pH 5.5 animals experienced a 65% loss in β_B (Table 2). Although the compensatory increase in β_A was almost negligible, the pH 5.5 animals still had significant reserves in β_A which are available in the case of a progressive acidosis (Figure 1B).

Heart rate (f_H), ventilation rate (f_A), and oxygen consumption rate ($\dot{M}_{O_2}$) were additionally monitored as diagnostic indicators for the mechanistic interpretation of acid-base disturbances. Compared to the control group, animals raised and tested under pH 6.0 showed a 20% higher f_H, a 14% higher f_A and a 38% higher $\dot{M}_{O_2}$ (Table 2), supposedly to meet the increased maintenance requirements for ion regulation. These systemic adjustments had no influence on extracellular P_{CO2}. The acidosis of the pH 6.0 animals (ΔpH = -0.16 units; Table 2) was therefore of metabolic rather than of respiratory origin. In agreement with the convention in acid-stress physiology [80], the term 'metabolic acidosis' is used here irrespective of whether the protons originate endogenously in connection with lactic acid production or exogenously, by the influx of H^+ down the large medium-to-hemolymph H^+ gradient. The metabolic acidosis was very likely caused by an influx of acidic equivalents from the ambient medium, since the sustained circulation and ventilation argue against the possibility of an activation of anaerobic support mechanisms.

Compared to the control group, the pH 5.5 animals experienced a 0.23-unit decrease in extracellular pH (Table 2), which can be characterized as metabolic acidosis with respiratory compensation as indicated by the reduced extracellular P_{CO2}. Since the oxygen consumption rate (and consequently the CO_2 production rate) did not change significantly in comparison to the control animals (Table 2), the main reasons for the reduced extracellular P_{CO2} are the 34–46% increased ventilation and perfusion rates (Table 2) as well as an enhanced permeability of the integument for respiratory gases, probably due to a thinner carapace. The latter explanation is consistent with the observation of the softer carapaces, which occurred only in the pH 5.5 animals. As in acid-stressed freshwater crayfish [81-83], the softer (jelly-like) carapace of pH 5.5 animals may indicate a poor calcification resulting from exoskeletal $CaCO_3$ erosion and reduced calcium and basic equivalent (HCO_3^-) uptake during the postmoult stage.

One may wonder why the acidification-induced increase in $\dot{M}_{O_2}$ was only present in the pH 6.0 animals but absent in the pH 5.5 animals. The $\dot{M}_{O_2}$ is expressed here as specific rate (nmol h^{-1} mm^{-3}), which is normalized to cubic body length rather than to body weight. It is common practice to estimate the body weight of daphnids from body length using scaling relationships (e.g. [84]).

However, we discarded this estimation because of the uncertainty about the influence of acidification on the relationship between body length and body weight. In the pH 5.5 animals, a reduction in the amount of metabolically active biomass (per cubic body length) could have masked the supposed extra costs for ion regulation. Evidence for this explanation comes from the comparison of brood sizes of those animals which were analyzed in the respiration experiment. The egg numbers of pH 5.5 animals (1.2 ± 0.6, range: 0–6, N = 12) were significantly lower than those of the pH 6.0 animals (9.1 ± 0.6, N = 12) and pH 7.8 animals (7.8 ± 1.0, N = 9) (Kruskal-Wallis test, $P < 0.001$). All eggs were of early developmental stage and accounted for very little respiration in the brooding females [85]. Nevertheless, the reduced allocation of resources into reproduction implies an acidification-induced disturbance in the energy and mass budgets of the pH 5.5 animals. Indeed, these animals showed the highest degree of transparency owing to the decreased appearance of orange-colored fat cells. Fat cells store carbohydrates and lipids [86-88], the latter in form of droplets which are usually colored, owing to the presence of carotinoids [89]. In addition, fat cells produce hemoglobin [90] and are supposed to be involved in vitellogenin synthesis [91]. Whether the acidification-induced disturbance in the energy and mass budgets results solely from the increased maintenance costs for ion homeostasis or, additionally, from a reduced assimilation rate (e.g. due suboptimal pH conditions for enzymatic digestion of food in the gut) needs further investigation.

It is important to note that no diapausing eggs occurred in pH 5.5 animals during the six-month experimental period. Obviously, the physiologically demanding condition of pH 5.5 was either not associated with an activation of the stress-signaling cascade responsible for production of male offspring [92,93] or males did not survive until maturity. The pH 6.0 animals, in contrast, were distinguished by the repeated occurrence of parthenogenic eggs with a white cover layer which probably resulted from a fungal infection. Although there are some reports on increased fungal parasitism in daphnids [94,95] and crayfish [82,96] under various stress conditions, it remains to be clarified whether acid stress leads to an increased susceptibility of daphnids to fungal parasites [97].

The role of acclimation in the tolerance to severe acid stress

The tolerance to a short-term exposure to severe acid stress (ambient pH 3–4) was examined in the control and acid-acclimated animals. The animals were initially exposed to their respective acclimation pH before the ambient pH was set to pH 4.0 and then to pH 3.0 (Figure 2). Upon exposure to ambient pH 4.0, all groups experienced an

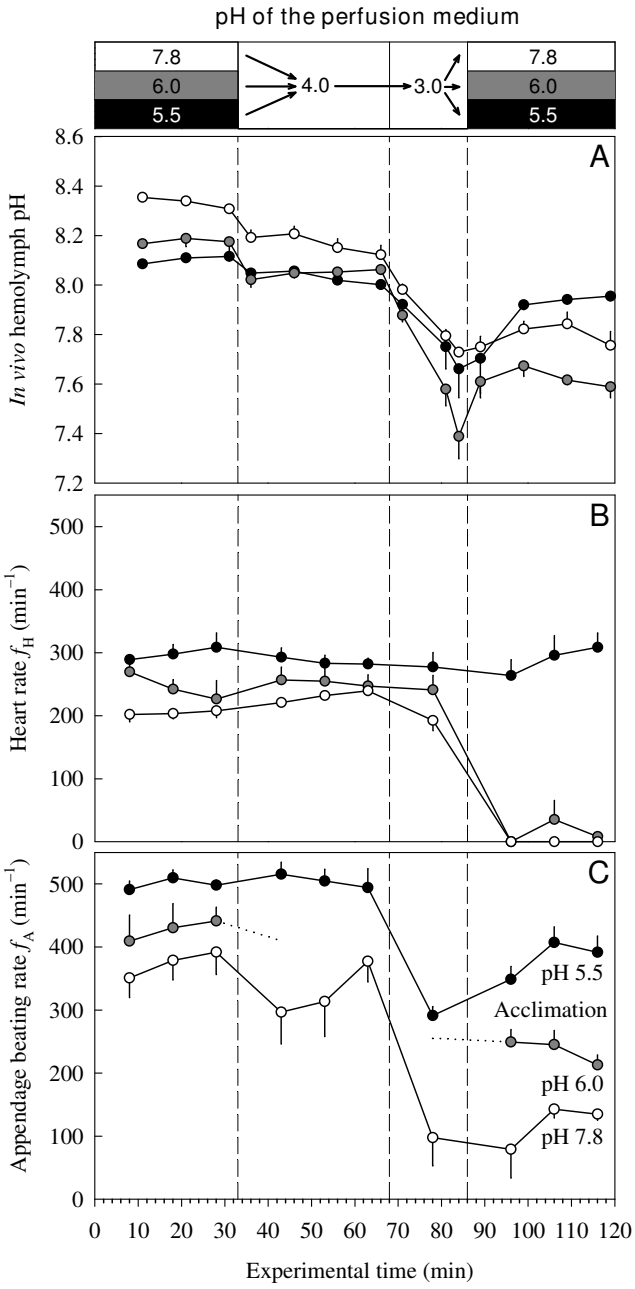

Figure 2
Tolerance to severe acid stress. Influence of ambient pH on *in vivo* hemolymph pH (A), heart rate (B) and appendage beating rate (C) of animals acclimated to pH 7.8 (open symbols), pH 6.0 (grey-filled symbols), and pH 5.5 (filled symbols). Data are given as means ± S.E. (N = 3–4). Dotted lines indicate a period of irregular limb beating activity. Each acclimation group was exposed to its acclimation pH during the initial and final phases of the experiment.

acidosis, but were able to stabilize their extracellular pH at a level 0.1–0.2 pH units below the respective pre-exposure value (Figure 2A). This response was caused by a 'metabolic acid load' of 7.0 meq L^{-1} (pH 7.8 animals), 4.5 meq L^{-1} (pH 6.0 animals), and 1.3 meq L^{-1} (pH 5.5 animals). While the f_H remained unaffected in all groups (Figure 2B), diverging responses were found in f_A (Figure 2C). The f_A response spectrum comprised a transient depression in pH 7.8 animals, an irregular beating behavior in pH 6.0 animals, and a sustained beating activity in pH 5.5 animals.

During the subsequent 18-min exposure to ambient pH 3.0, the pH homeostasis collapsed in all acclimation groups. The extracellular pH showed a progressive decline (Figure 2A), which corresponded to a net flux of acidic equivalents from the ambient medium into the hemolymph of 32 meq L^{-1} h^{-1} (pH 7.8 animals), 46 meq L^{-1} h^{-1} (pH 6.0 animals), and 16 meq L^{-1} h^{-1} (pH 5.5 animals). This massive net influx of acidic equivalents is in line with reports on the breakdown of ion regulation [34,35,98,99]. In *D. magna*, severe acid stress resulted in a 60–70% inhibition of the unidirectional sodium influx and a 130% increase in sodium outflux [34]. Within one hour, these animals lost 30–50% of their body sodium. The whole-body sodium concentration of *D. magna* is 26–41 mmol (kg wet mass)$^{-1}$ [35,98,100,101], assuming a wet-to-dry mass ratio of 10:1 [102]. This whole-body concentration is consistent with a hemolymph concentration of 65 mM sodium [103], taking into account that the hemolymph comprises 60% of the body volume [102] and that the extracellular fluid contains the main portion of whole-body sodium. The estimated net efflux of sodium (20–30 mmol L^{-1} h^{-1}) from the hemolymph of *D. magna* compares well with the net influx of acidic equivalents into the hemolymph of *D. pulex* (32 meq L^{-1} h^{-1} in control animals). This shows that the disturbance in acid-base balance mirrors the disturbance in ion regulation and vice versa.

During the exposure to ambient pH 3.0, the f_A decreased strongly in all groups, whereas f_H remained apparently unaffected (Figure 2B, C). However, the subsequent recovery period revealed a (somewhat delayed) heart arrest and a deformation of heart structure in the pH 7.8 and pH 6.0 animals. Their extracellular pH values during the recovery period remained 0.55 pH units below initial (pre-acid exposure) values. The pH 5.5 animals, in contrast, were able to reduce the difference between the pre- and post-exposure values to 0.16 units. This was the only group which survived the severe-acid test.

Of all acclimation groups, the pH 5.5 animals had the highest tolerance to severe acid stress as indicated by the lowest net influx of acidic equivalents (16 meq L^{-1} h^{-1}). This implies a lower disturbance of extracellular ion regulation in the pH 5.5 animals compared to the other two acclimation groups, which may explain the unique ability to sustain heart-beating activity in the former and heart arrest in the latter. The results of the severe-acid test further suggest that the acclimation to ambient pH 5.5 induced a compensatory increase in active ion transport and/or a reduction in the epithelial permeability for sodium and hydrogen ions. However, the suggested reduction in epithelial ion permeability contrasts with the increased integumental permeability for respiratory gases arising from the impaired carapace formation. It therefore seems that active compensation in ion transport is the more likely defence mechanism.

Interdependence between acid-base balance and CO_2 transport

Information on extracellular pH in the heart region and on hemolymph bicarbonate concentration made it possible to determine the local P_{CO2} in the pericardial hemolymph. In daphnids, the pericardial space receives hemolymph from the carapace lacuna, which is an important site of gas exchange [36,76], and from the dorsal lacuna, which is fed by the current leaving the intestinal lacuna [36]. In the carapace lacuna, the P_{CO2} is low due to the transintegumental diffusion of CO_2 from the hemolymph into the ambient medium. In the intestinal lacuna (which traverses the body core region), the P_{CO2} is high because metabolically produced CO_2 is released into the hemolymph. The local P_{CO2} in the pericardial space therefore assumes an intermediate value that lies between the two P_{CO2} extremes. The magnitude of the P_{CO2} differences in the circulatory system strongly depends on the presence or absence of a carbonic anhydrase (CA). In the absence of a CA, the interconversion between CO_2 and HCO_3^- proceeds slowly [104]. For example, a 25 mM bicarbonate solution with a non-bicarbonate buffer value of 2–10 meq L^{-1} pH^{-1} needs 3–12 s for a half-change in hydrogen concentration following the abrupt increase in P_{CO2} from 5 to 11 kPa [105]. These half-equilibration times apply to 37°C, so even longer would be needed at 20°C. Given a hemolymph circulation time of 21 s in a 2.5 mm *D. magna* at 20°C (cardiac output: 32 nl s^{-1} [74], hemolymph volume: 680 nl [102], it is clear that hemolymph passage time from the tissues to the respiratory surfaces is too short to bring the uncatalyzed $CO_2+H_2O \leftrightarrow H^+ + HCO_3^-$ reaction into *full* equilibrium. Under these circumstances, the main share of metabolically produced CO_2 would be transported as physically dissolved gas rather than in the

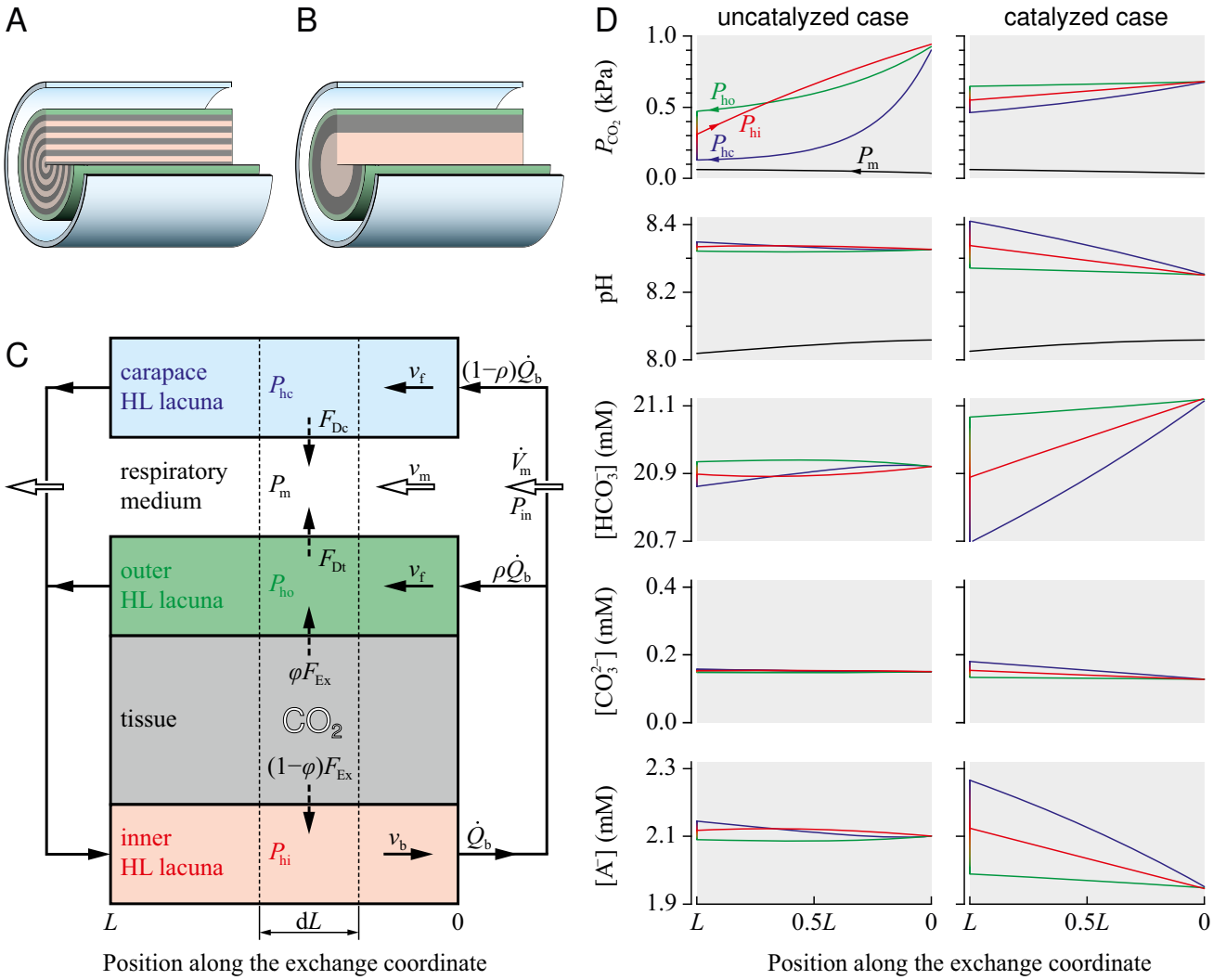

Figure 3

Modelling and simulation of CO_2 transport. (A) Reference topology based on a cylinder-within-tubes arrangement (R. Moenickes, O. Richter and R. Pirow, in preparation). A sector piece was removed to show the alternation of concentric hollow cylinders of tissue (gray) and hemolymph (red, green, blue). (B) Simplified topology with only one tissue layer. This topology is applied in the compartment model. (C) Compartment model of the relevant transport processes. CO_2 is excreted from the tissue compartment of length d*L* into the inner and outer hemolymph (HL) lacuna at rates of $(1-\phi)F_{Ex}$ and ϕF_{Ex}. Hemolymph leaving the inner HL lacuna at a volume-flow rate $\dot{Q}_b$ is distributed between the outer HL lacuna and the carapace HL lacuna. From these compartments CO_2 diffuses across cuticular barriers into the medium, which flows at a rate of $\dot{V}_m$. Indicated are the CO_2 partial pressures (P_{hi}, P_{ho}, P_{hc}, P_m) and flow velocities (v_b, v_f, v_m) in the hemolymph lacunae and the medium. P_{in} is the inspiratory P_{CO2}. (D) Simulation results for the uncatalyzed and catalyzed hydration of CO_2 for an animal exposed to normal conditions (ambient pH = 8.0, ambient P_{CO2} = 0.035 kPa). Acid-base variables are shown for the medium and hemolymph lacunae in relation to the exchange coordinate.

chemically combined form as bicarbonate with the consequence of relatively large P_{CO2} differences between the loading and unloading sites.

Knowledge about the presence or absence of a CA in the circulatory fluid is therefore fundamental for the understanding of CO_2 transport and acid-base balance in daphnids. The reported absence of CA activity in the hemolymph of decapod crustaceans [106-109] prompted us to analyse the physiological implications of circulatory CO_2 transport under uncatalyzed conditions in more detail. Based on established concepts of compartment modelling [110,111] and on own experiences in the simulation of whole-animal oxygen transport in daphnids [71,112], we derived a multi-compartment model of the CO_2 diffusion-convection-reaction system (Figure 3C) to simulate the transport of CO_2 from the tissue *via* the hemolymph to the ambient medium. To obtain a pH of 8.334 at the entrance of the inner hemolymph lacuna (Figure 3C), the Krogh constant for the diffusion of CO_2 in chitin (K) was set to 2.10×10^{-6} nmol s^{-1} mm^{-1} kPa^{-1}. To our knowledge, there are no experimental data in the literature on Krogh's diffusion constant for CO_2 in chitin. Nevertheless, the chosen K value is plausible insofar as it is of the same order of magnitude as Krogh's diffusion constant for O_2 in chitin (0.95×10^{-6} nmol s^{-1} mm^{-1} kPa^{-1}) [113]. The similarity in both values seems to contradict the well-known fact that Krogh's diffusion constant for CO_2 in water and aqueous tissues is 20–25 times higher than that for O_2, a phenomenon that is explained by the higher capacitance (solubility) coefficient of CO_2 in *aqueous* media [114]. The cuticle of arthropods, however, is primarily composed of chitin fibers which are embedded in a more or less hydrated protein matrix [115]. Among the different layers (epicuticle, exocuticle, endocuticle), the exocuticle is relatively *dehydrated* [115] and may therefore establish a similar diffusion barrier for O_2 and CO_2.

The CO_2 transport model made it possible to follow the changes in extracellular acid-base variables during a full circulation cycle (Figure 3D, uncatalyzed case). The extracellular P_{CO2} in the three hemolymph compartments varies largely between 0.13–0.94 kPa, whereas the extracellular pH remains confined to the narrow range of pH 8.32–8.35. The small changes in bicarbonate concentration (< 0.01 mM) reflect the slow interconversion between CO_2 and HCO_3^-. Compared to bicarbonate, the carbonate and non-bicarbonate buffers show concentration changes in opposite direction as they are involved in the buffering of hydrogen ions arising from the hydration of CO_2 and subsequent dissociation of carbonic acid.

The simulation provides a plausible prediction of the extracellular CO_2 and pH gradients that would develop in the absence of a hemolymph CA. However, a screening of the *D. pulex* genome database [116,117] unexpectedly revealed 31 genes with CA-like coding sequences (Table 4). These genes belong to two evolutionarily unrelated CA gene families (α-CA and β-CA) [118]. The derived amino-acid sequences were aligned with selected metazoan sequences (Additional files 1 and 2) [119-122] and classified in terms of their putative destination (Figure 4A, B) [123], based on sequence features and the known localization of CAs from crab [124], mosquito [125], and man [118]. The phylogenetic analysis of α-CA sequences showed a distinct separation between mitochondrial and cytoplasmic, CA-related, membrane-bound and transmembrane, and secretory proteins (Figure 4A). Among the 30 α-CAs from *D. pulex* were 25 sequences (CAA6A-H, CAA7A-Q) with an N-terminal signal peptide for secretory export. Seven of these putative extracellular isoforms are currently supported by EST data. So far, nothing is is known about the extracellular target sites. To account for the possibility of CA secretion into the hemolymph, we simulated a second scenario, in which a hemolymph CA accelerates the interconversion between CO_2 and HCO_3^- by a factor of 10000 [126], which is sufficiently large to establish an equilibrium. Krogh's diffusion constant for CO_2 in chitin was slightly reduced to 1.30×10^{-6} nmol s^{-1} mm^{-1} kPa^{-1} to obtain a pH of 8.334 at the entrance of the inner hemolymph lacuna (Figure 3C). Compared to the uncatalyzed case, the catalyzed hydration/dehydration of CO_2 significantly reduced the variations in extracellular P_{CO2} to the narrow range of 0.46–0.68 kPa (Figure 3D), indicating that less CO_2 is transported as physically dissolved gas. Instead, more CO_2 is transported in the chemically combined form as reflected by the large variation in bicarbonate concentration. Moreover, the extracellular pH varied substantially between the 'prebranchial' value of 8.25 (inner HL lacuna) and the 'postbranchial' value of 8.41 (carapace HL lacuna).

The two simulated scenarios represent a coherent description of the physiological implications arising from the presence or absence of a CA in the hemolymph of *D. pulex*. The selected values for the global adjustment parameter K remain within reasonable bounds that made it impossible to put more weight to one of the two models. Nevertheless, the predicted extracellular P_{CO2} and pH gradients represent a working hypothesis that will be tested in subsequent experiments. pH imaging tech-

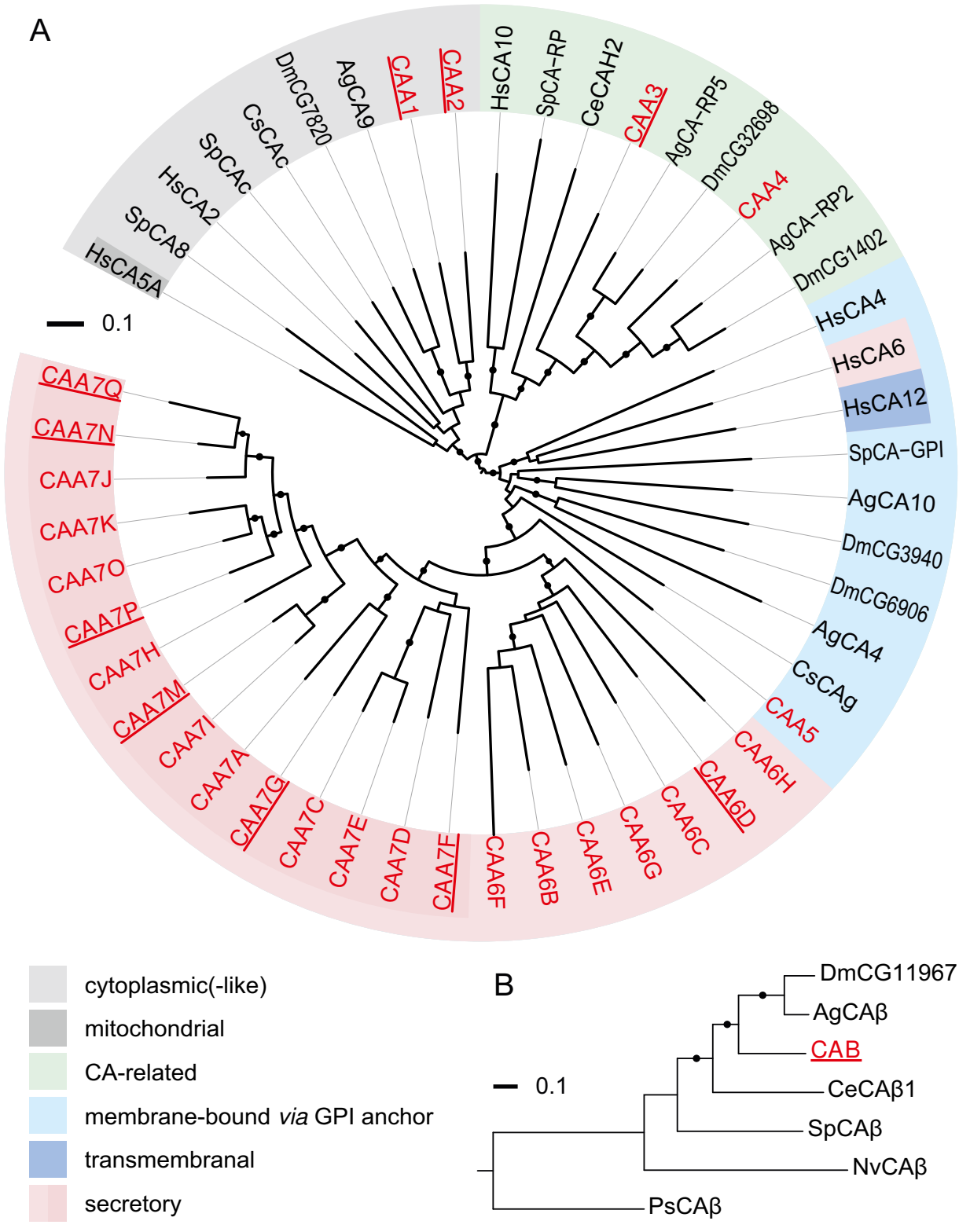

Figure 4 *(see legend on next page)*

Figure 4 *(see previous page)*
Classification of CA-like amino acid sequences from *Daphnia pulex*. Phylogenetic trees for selected α-carbonic anhydrases (α-CAs) (A) and β-CAs (B) based on multiple-sequence alignments (Additional files 1 and 2). *D. pulex* sequences are shown in red; underlined labels indicate EST support. Three fragmentary sequences (CAA6A, CAA7B, CAA7L; Table 4) from *D. pulex* were excluded from the alignment. Additionally included were related sequences from the blue crab *Callinectes sapidus* (Cs), *Drosophila melanogaster* (Dm), *Anopheles gambiae* (Ag), *Caenorhabditis elegans* (Ce), sea urchin *Strongylocentrotus purpuratus* (Sp), *Homo sapiens* (Hs), the sea anemone *Nematostella vectensis* (Nv), and *Pisum sativum* (Ps). α-CAs were classified in terms of their putative destination into mitochondrial and cytoplasmic, CA-related, membrane-bound and transmembrane, and secretory proteins. CA-related proteins have lost most of the highly conserved active-site residues. Membrane-associated α-CAs have a C-terminal attachment signal for a glycosylphosphatidylinositol (GPI) anchor which tethers the extracellular protein to the cell membrane [123]. The trees were constructed using the neighbor-joining algorithm. Bootstrap analysis was performed with 1000 replicates (bootstrap values > 800 are indicated by filled circles). For sequence references, see Additional files 1 and 2.

niques, for example, should have the resolution power to detect a spatial *in vivo* gradient as large as 0.1–0.2 pH units to verify or falsify the assumption of CA activity in the circulatory system of *D. pulex*. Further *in vivo* experiments may include the application of a strong diffusible CA inhibitor or the microinjection of an exogenous CA [127].

Conclusion

Chronic acid exposure induced pronounced effects in extracellular pH, bicarbonate concentration and CO_2 partial pressure, as well as in circulation, ventilation and energy metabolism. Compensatory changes in extracellular non-bicarbonate buffering capacity and the improved tolerance to severe acid stress indicated the activation of defense mechanisms. The physiological changes were associated with an impairment of carapace formation and with reductions in reserve materials and reproduction. Mechanistic analyses of the interdependence between extracellular acid-base balance and CO_2 transport led to the identification and classification of 31 carbonic anhydrase isoforms which are encoded in the genome of *D. pulex*. The multitude of physiological information that can be acquired from these transparent crustaceans *via* optical techniques underlines the great advantage of *Daphnia pulex* as a model system for environmental studies. Proteomic analyses are underway to identify the molecular mechanisms and target genes involved in *Daphnia's* responses to a variety of environmental stresses including freshwater acidification.

Methods

Acclimation conditions

Animals were raised at 20°C in aerated M4 medium [128] under three different pH conditions at a 16 h:8 h L:D photoperiod. The control condition (7.8 ± 0.2, mean ± variation range) was manually adjusted twice a week using 0.005 M H_2SO_4 and 0.01 M NaOH. The pH 6.0 ± 0.1 condition was established by adding 5 mM MES buffer (2-morpholinoethansulfonic acid) to the medium. pH 5.5 ± 0.05 was maintained by a pH-Stat, which was equipped with a pH electrode (N 6000; Schott-Geräte GmbH, Mainz, Germany) and which controlled the addition of 0.05 M H_2SO_4 delivered by a peristaltic pump (Gilson ABIMED, Villiers, France).

The pH 7.8 and pH 6.0 animals were cultured in 2 L glass beakers (containing 1.8 L medium) at a density of 25–50 individuals (juveniles plus adults) per vessel. The pH 5.5 animals were kept in a 20 L glass aquarium (containing 8 L medium) at a density of 100–200 individuals. Surplus offspring were sorted out twice a week. Given the case of appearance, females with ephippia and males were sorted out, so that parthenogenesis and clonal reproduction was maintained. Animals were fed *ad libitum* with *Desmodesmus subspicatus* (final concentration: 15.5×10^4 cells per ml culturing medium) six times a week. To minimize the influence of algae on medium pH [129], sedimented food material was removed once (glass aquarium) or twice (glass beaker) a week. During this procedure, any algal surface buildup was removed by scrubbing the enclosures, and at least half of the medium was exchanged by fresh medium.

Analysis of hemolymph buffer curves

Hemolymph samples (0.2–1 μl per animal) were drawn as described elsewhere [73] and collected in ice-cooled 500 μl reaction vials. The pooled hemolymph (30–100 μl) was filtered (cellulose acetate syringe filters, 0.45 μm pore size; Nalgene, Rochester, NY), shortly centrifuged to remove any air bubbles, and finally kept on ice. Hemolymph buffer curves were measured with a micro-pH-electrode (MI-4152; Microelectrodes Inc., Bedford, U.S.A.) in a gas diffusion chamber [130] at 20°C. The pH electrode was linked to a pH-meter (MP 230, Mettler Toledo, Swiss) which transferred the data to a computer. Traceable NIST standard reference buffers (pH 6.88 and pH 9.23 at 20°C, type number: L 4798; Schott-Geräte GmbH) were used for calibration. Hemolymph samples of 5–10 μl were equilibrated with humidified gas mixtures of different CO_2 partial pressure (P_{CO2} = 0.135–5.50 kPa). The gas mixtures

Table 4: List of referred carbonic anhydrase-like proteins and gene models from *D. pulex*.

Symbol	Model name	Protein ID	Reference ID
CAB	PIR_PASA_GEN_2900003	347880	304414
CAA1	PIR_estExt_fgenesh1_pg.C_80063	442498	222096
CAA2	PIR_estExt_fgenesh1_pg.C_80158	442497	222141
CAA3	PIR_e_gw1.74.6.1	442499	58540
CAA4	PIR_e_gw1.4.553.1	442496	42376
CAA5	PIR_NCBI_GNO_2000180	442477	317362
CAA6A	PIR_1_NCBI_GNO_0400291	442779	311517
CAA6B	PIR_SNAP_00002730	442471	41941
CAA6C	PIR_e_gw1.4.143.1	442472	41941
CAA6D	PIR_PASA_GEN_0400293	442467	305654
CAA6E	PIR_NCBI_GNO_0400294	442475	311520
CAA6F	PIR_e_gw1.4.154.1	442468	42212
CAA6G	PIR_e_gw1.4.906.1	442476	42004
CAA6H	PIR_e_gw1.4.98.1	442478	42484
CAA7A	PIR_PASA_GEN_0400138	442480	305530
CAA7B	PIR_NCBI_GNO_0400455	442481	42005
CAA7C	PIR_SNAP_00002914	442482	none
CAA7D	PIR_SNAP_00002915	442483	42005
CAA7E	PIR_NCBI_GNO_0400456	442484	42005
CAA7F	PIR_PASA_GEN_0400354	442479	305707
CAA7G	PIR_PASA_GEN_3600071	442494	305268
CAA7H	PIR_SNAP_00002923	442485	234865
CAA7I	PIR_NCBI_GNO_0400466	442486	42371
CAA7J	PIR_e_gw1.4.668.1	442487	42371
CAA7K	PIR_SNAP_00002925	442488	234867
CAA7L	PIR_SNAP_00002926	442489	234868
CAA7M	PIR_NCBI_GNO_0400472	442491	221343
CAA7N	PIR_estExt_fgenesh1_pg.C_40469	442490	221343

Table 4: List of referred carbonic anhydrase-like proteins and gene models from *D. pulex*. *(Continued)*

CAA7O	PIR_NCBI_GNO_0400474	442492	311700
CAA7P	PIR_estExt_Genewise1.C_40740	442493	207081
CAA7Q	PIR_estExt_fgenesh1_pg.C_400146	442495	225703

Given are the protein names, gene model names and protein identification numbers of those loci which were annotated in the present study. Protein IDs indicate manually curated gene models that may differ from those contained in the 'Filtered Models v1.1' set (released by JGI in July 2007) [117]. The Reference ID can be used to retrieve the corresponding models from the Filtered Models set v1.1.

were prepared from highly pure nitrogen (> 99.996%) and carbon dioxide (99.995%; Air Liquide, Düsseldorf, Germany) using a gas mixing pump (2 M 303/a-F Wösthoff oHG Bochum, Germany).

For analysis, the hemolymph of *Daphnia* was considered as a binary buffer system consisting of the carbonate system and a monoprotic non-bicarbonate buffer ($HA \leftrightarrow H^+ + A^-$). The dependence of pH on P_{CO2} for such a system is described by the following balance equation [131]

$$0 = \alpha_{CO_2} P_{CO_2} \left(\frac{K'_1}{\{H^+\}} + \frac{2K'_1K'_2}{\{H^+\}^2} \right) + \frac{K'_W}{\{H^+\}} + \frac{C_A}{\{H^+\}/K'_A + 1} - \{H^+\} - SID, \quad (1)$$

where $\{H^+\}$ is 10^{-pH}, K'_w (= 10^{-14} M) is the dissociation equilibrium constant of water, and SID represents the strong ion difference [132]. C_A and K'_A are the concentration and dissociation equilibrium constants of the non-bicarbonate buffer, whereas K'_1 and K'_2 represent the first and second dissociation equilibrium constants of the carbonate system. The physical solubility of CO_2 in hemolymph (α_{CO2} = 0.3682 mmol l^{-1} kPa^{-1}) was calculated according to a thermodynamic model [133,134], assuming a sodium concentration of 58 mM and a solution density of 1 g l^{-1}. Operational p*K*'-values of the carbonate system (pK'_1 = 6.325 ± 0.002, pK'_2 = 10.47 ± 0.09; means ± S.E.) were determined from standard bicarbonate solutions (4, 8, 16 mM $NaHCO_3$ plus 50 mM NaCl) using three equilibration steps (P_{CO2} = 0.13, 0.50, 2.0 kPa) (Additional file 3). These standard bicarbonate solutions were a valid representation of *Daphnia* hemolymph in terms of ionic strength which, besides protein concentration, affects the α_{CO2} and the p*K*'-values [131]. The influence of protein concentration on α_{CO2} was negligible because the proteins in *Daphnia* hemolymph occupy less than 1% of hemolymph volume.

Given the P_{CO2}-pH data, parameter values for SID, C_A and K'_A were obtained by nonlinear least-squares data fitting. The analytical procedure additionally contained a correction for incomplete hemolymph equilibration at the lowest P_{CO2} step (Additional file 3). The concentrations of bicarbonate and carbonate are given by

$$[HCO_3^-] = \alpha_{CO_2} P_{CO_2} 10^{pH - pK'_1} \quad (2)$$

and

$$[CO_3^{2-}] = [HCO_3^-] \cdot 10^{pH - pK'_2}. \quad (3)$$

The appropriateness of the operational parameter values for the calculation of bicarbonate was validated by the direct measurement of total CO_2 in *Triops cancriformis* hemolymph (R. Pirow, unpublished data), whose ionic strength is comparable to that of *Daphnia* hemolymph. The non-bicarbonate buffer value (β_A) was obtained from [131,135]

$$\beta_A = \ln 10 \cdot C_A \frac{K'_A \{H^+\}}{\left(K'_A + \{H^+\}\right)^2}. \quad (4)$$

The buffer values of bicarbonate (β_B) and carbonate (β_C) were determined for the open-system condition [135,136], under which the hemolymph P_{CO2} is assumed to be held constant *in vivo* (as by the control of ventilation) [136]:

$$\beta_B = \ln 10 \cdot [HCO_3^-] \quad (5)$$

and

$$\beta_C = 2 \cdot \ln 10 \cdot [CO_3^{2-}]. \quad (6)$$

Finally, the concentration of acidic equivalents added to the hemolymph (ΔH^+, 'metabolic acid load') [78] during acute exposure to severe acid stress was obtained from

$$\Delta H^+ = [HCO_3^-]_1 - [HCO_3^-]_2 + [HA]_2 - [HA]_1, \quad (7)$$

where the subindices 1 and 2 refer to the concentrations before and during the exposure.

Microfluorometric set-up

Fluorescence measurements were performed with an inverted microscope (Axiovert 10, Carl Zeiss, Oberkochen, Germany) equipped with a monochromatic illumi-

nation system (T.I.L.L. Photonics, Planegg, Germany) and an imaging spectrograph (SpectraPro-275I, Acton Research Corporation, Acton, MA, USA). A 10 × objective (Plan Neofluar, Zeiss) was used for all experiments. The fluorescence light was transmitted by a quartz fibre-optic light guide to the imaging spectrograph, which was equipped with a thermoelectrically-cooled (-10°C) CCD camera (HLS 1024/64bi; Proscan elektronische Systeme GmbH, Lagerfeld, Germany) containing a highly-sensitive (back-thinned), 16-bit CCD chip (1024 × 58 pixels; S7031-1006, Hamamatsu Photonics, Herrsching am Ammersee, Germany). A CCD exposure time of 2 min was used for spectrum acquisition. Fluorescence emission spectra were smoothed with a span of 30 nm.

Calibration of cSNARF-1

A stock solution of 70-kDa dextran-coupled cSNARF-1 (D-3304, Molecular Probes, Inc., Oregon, USA) was prepared by dissolving 5 mg lyophilized dye in 250 µl sterile-filtered Milli-Q water (Millipore, Schwalbach, Germany). The stock solution was 1:20 diluted with a 10 mM $NaHCO_3$ solution containing 50 mM NaCl. Given a conjugation ratio of 3–8 chromophore groups per dextran particle (Molecular Probes product information, 2003), the average concentration of cSNARF-1 in the calibration solution was 80 µM. Using the diffusion chamber and the microfluorometric set-up described above, a 10 µl sample was equilibrated with gas mixtures of different P_{CO2} (0.135–5.50 kPa). At the end of each equilibration step, a fluorescence spectrum and the sample pH were measured.

The CO_2 titration of a bicarbonate-buffered cSNARF-1 solution containing additionally 50 mM NaCl had the advantage of calibrating the pH-sensitive dye in a chemical environment whose ionic composition is similar to that of *Daphnia* hemolymph (see Discussion). However, the chosen CO_2 partial pressures were not sufficient to achieve pH extremes which could shift the dye into the fully protonated (acid) and deprotonated (base) forms (Figure 5A). Reiterative least-squares spectral resolution (Additional file 4) [137] was therefore employed to recover the spectra of the acid/base forms (Figure 5B) and the pK'_a value of cSNARF-1. The calibration yielded a pK'_a of 7.624 (Figure 5D).

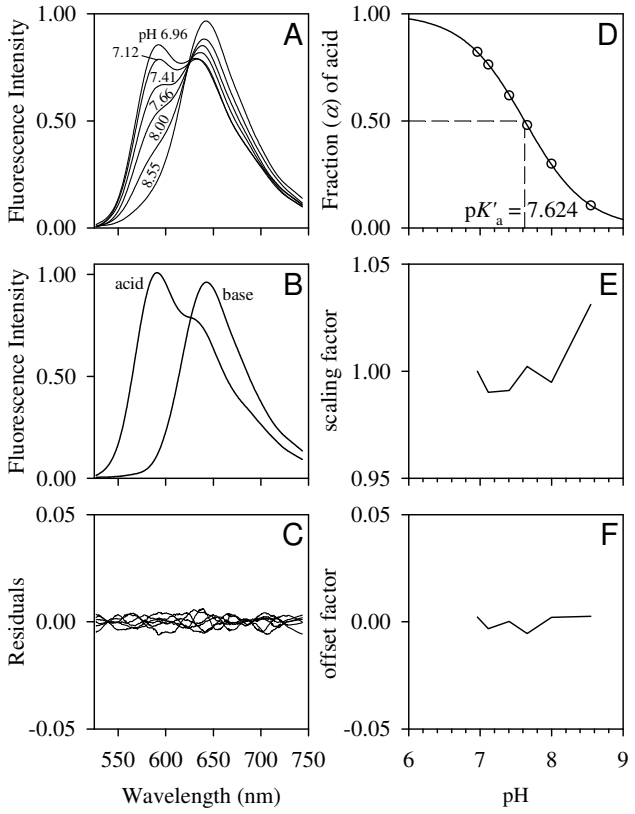

Figure 5

Calibration of cSNARF-1. Fluorescence emission spectra of a bicarbonate-buffered cSNARF-1 solution were acquired at various pH values (A). Fluorescence excitation was at 475 nm. Reiterative least-squares spectral resolution [137] (Additional file 4) was applied to the data to extract the spectra of the acid/base forms (B) and the pK'_a value of cSNARF-1. The underlying model that relates the fraction of acid α to pH (D) is given by $\alpha = \{H^+\}/(K'_a + \{H^+\})$. The optimum pK'_A value of 7.624 was reiteratively obtained by using the Nelder-Mead simplex algorithm [144]. The inclusion of an additive offset factor (E) and multiplicative scaling factor (F) into the optimization corrected for variations in CCD dark current, excitation light intensity, sample shape, and fluorophore concentration. The residuals (C) represent 'unexplained' spectral information (noise).

In vivo *measurements*

Adult females with a carapace length of 1.9–2.6 mm and parthenogenetic embryos of developmental stage 2 [138] were used. Animals were immobilized as described [73]. For cSNARF-1 microinjection, small glass capillaries (GB 120 F10, Science Products GmbH, Hofheim, Germany) were thinly drawn out with a micropipette puller (model 77; Sutter Instruments, Novato, CA, USA). 2 µl cSNARF-1 stock solution (1.57 mM) were loaded into the micropipette. The solution was microinjected (Transjector 5246; Eppendorf, Hamburg, Germany) through the basal joint membrane of one of the large antennae into the hemolymph space. The injection was followed using a stereomicroscope (SZH-ILLK; Olympus GmbH, Hamburg, Germany). After 2–6 hours of recovery in nutrient-free medium, the animal was transferred into a perfusion chamber as described elsewhere [73]. The flow rate of the perfusion medium was maintained at 5.5 ml min^{-1} using a peristaltic pump (MCP Standard ISM 404; Ismatec SA, Glattbrugg, Swiss). The initial pH of the perfusion

medium corresponded to the acclimation pH of the animals. During the experiment, the animal was exposed to a stepwise variation in ambient pH using the following sequence: initial (acclimation) pH (33 min), pH 4.0 (35 min), pH 3.0 (18 min), and acclimation pH (34 min). All perfusion media were buffered using 5 mM HEPES (pH 7.8), 5 mM MES (pH 6.0), or 5 mM citrate (pH 5.5, 4.0, 3.0). The medium pH was continuously controlled using a pH electrode (N 6000). During the experiment, the fluorescence-spectrum acquisition alternated with the acquisition of video images of the animal under infrared transillumination. From these video sequences, the heart rate and appendage beating rate was determined by digital motion analysis as described elsewhere [73].

Analysis of in vivo *cSNARF-1 spectra*

cSNARF-1 fluorescence spectra were obtained from the hemolymph space around the heart region. Since all tested animals were in a fasting state, the *in vivo* spectra did not contain any noticeable contributions from ingested autofluorescing algae which, if present, would have seriously affected the pH determination. The excellent quality of the *in vivo* cSNARF-1 spectra (Figure 6A) made it possible to determine the *in vivo* pH with high precision using multicomponent analysis (Additional file 4) [139]. Since the *in vivo* spectra could not be fitted by the calibration spectra (Figure 5B), probably due to a calibration-inherent distortion of the acid spectrum around 600–700 nm, new acid/base spectra of cSNARF-1 were measured in *Daphnia magna* hemolymph. The hemolymph samples were acidified by equilibration with 100% CO_2 gas and basified by the addition of NaOH under CO_2-free gas conditions (100% N_2). As a modification to the calibration experiment, the micro-pH-electrode was not inserted into the hemolymph samples to avoid any optical interferences. The obtained acid/base spectra (Figure 6B) were finally scaled to the peak-to-peak ratio of the calibration spectra (Figure 5B). The multicomponent analysis determined the fractional contribution (α) of the acid form of cSNARF-1 to the *in vivo* spectra. The pH was finally calculated from α and the pK'_a value of cSNARF-1 (Figure 6D) according to

$$\mathrm{pH} = pK'_a + \log_{10}\frac{\alpha}{1-\alpha}. \qquad (8)$$

Respiration measurements

The oxygen consumption rate ($\dot{M}_{O_2}$) of a group of 3–4 animals (2.0–3.3 mm body length) carrying parthenogenetic embryos of developmental stage 1–2 [138] was measured at 20°C as described elsewhere [74]. The respiratory medium consisted of M4 medium containing 10 mM buffer (HEPES: pH 7.8, MES: pH 6.0, citrate: pH 5.5). Tetrazyclin and Streptomycin (12.5 mg l^{-1} each) was added to reduce bacterial respiration. The specific oxygen consumption rate was obtained by dividing the whole-animal oxygen consumption rate by the cubic body length.

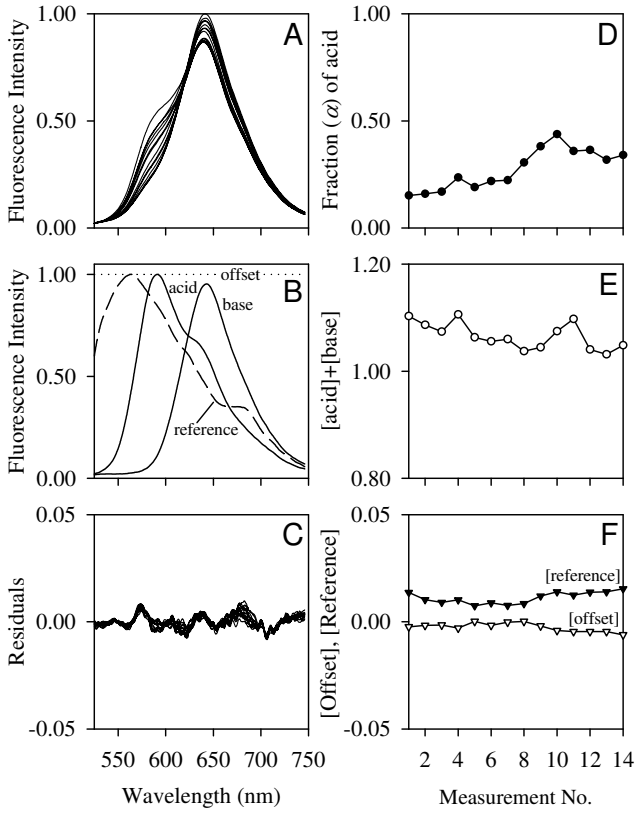

Figure 6

Analysis of *in vivo* cSNARF-1 spectra. Example *in vivo* spectra (A) from a pH 7.8 acclimated *Daphnia pulex* exposed to ambient pH 7.8-3.0. The corresponding pH values were retrieved by a multicomponent analysis [139] (Additional file 4), which determines the composition of a mixture of components, given that the spectrum of each component is known. The component spectra (B) comprised the *in vitro* spectra of the acid/base forms of cSNARF-1 (measured in *Daphnia* hemolymph), a reference (autofluorescence) spectrum from non-injected animals, and an offset (background) spectrum. The multicomponent analysis yielded the fraction of the acid form (D), the relative chromophore (acid plus base) concentration (E), as well as the contributions of the reference and offset signals (F). The residuals (C) represent spectral information that could not be explained by the component signals.

Modelling of whole-animal CO_2 transport

A topological model was derived from a geometric concept on convective-diffusive oxygen transport in daphnids [71,112]. In this concept, the animal's complex body is reduced to a cylindrical trunk which is wrapped by a hol-

low cylinder representing the carapace (Figure 3A). The carapace is a double-walled, hollow structure that is perfused with hemolymph. The hollow-cylindric space between the carapace and the trunk is occupied by the respiratory medium. As a simplification of the reference model (Figure 3A), the present model is composed of only five subdomains (Figure 3B). These are the inner hemolymph lacuna, a single tissue layer, the outer hemolymph lacuna, the respiratory medium, and the carapace hemolymph lacuna, as outlined in the conceptual overview of the compartment model (Figure 3C). Each subdomain has a total length L and is divided into N compartments of length dL.

The processes operating within each compartment and in between adjacent/connected compartments include (i) the excretion of CO_2 from tissue into hemolymph, (ii) the CO_2 hydration and acid-base reactions in hemolymph and medium, (iii) the convective transport of reaction species, and (iv) the diffusive transport of CO_2 across cuticular barriers. A mathematical formulation of the physico-chemical processes is given for a single compartment of the outer hemolymph lacuna. For compartments of other subdomains, equations can be derived in an analogous manner.

(i) The rate (nmol s^{-1}) at which CO_2 is excreted from a tissue compartment of thickness dL into the outer hemolymph lacuna is ϕF_{ex} with

$$F_{Ex} = \dot{M}_{CO_2}\, dL/L\,, \tag{9}$$

where $\dot{M}_{O_2}$ is the whole-animal CO_2 production rate. The factor ϕ is the fraction of excreted CO_2 that is released into the outer hemolymph lacuna. The remaining fraction (1-ϕ) is received by the inner hemolymph lacuna.

(ii) The hydration and subsequent dissociation of CO_2, its combination with OH^-, and the dissociation of bicarbonate and the non-bicarbonate buffer HA are given by

$$CO_2 + H_2O \underset{\mu\cdot k_1/K_1'}{\overset{\mu\cdot k_1}{\rightleftharpoons}} H^+ + HCO_3^-$$

$$HCO_3^- \underset{k_2}{\overset{k_2/K_2'}{\rightleftharpoons}} H^+ + CO_3^{2-}$$

$$CO_2 + OH^- \underset{k_{-3}}{\overset{k_3}{\rightleftharpoons}} HCO_3^-$$

$$HA \underset{k_4}{\overset{k_4/K_A'}{\rightleftharpoons}} H^+ + A^-$$

The lower and upper-case ks represent kinetic and thermodynamic constants (Table 5), whereas μ is the factor by which the uncatalyzed interconversion between CO_2 and HCO_3^- is accelerated in the presence of a carbonic anhydrase. The turnover rates (mol L^{-1} s^{-1}) of the forward and backward reactions are defined as

$$R_1 = \mu k_1 [CO_2] \tag{10}$$

$$R_{-1} = \mu\, k_1/K_1' \{H^+\}[HCO_3^-] \tag{11}$$

$$R_2 = k_2/K_2' [HCO_3^-] \tag{12}$$

$$R_{-2} = k_2 \{H^+\}[CO_3^{2-}] \tag{13}$$

$$R_3 = k_3 \cdot K_w' [CO_2] / \{H^+\} \tag{14}$$

$$R_{-3} = k_{-3}[HCO_3^-] \tag{15}$$

$$R_4 = k_4/K_A' [HA] \tag{16}$$

$$R_{-4} = k_4 \{H^+\}[A^-] \tag{17}$$

The hydrogen activity, $\{H^+\}$, was calculated from hydrogen concentration as $\{H^+\} = \gamma_H [H^+]$. The H^+ activity coefficient ($\gamma_H = 0.797$) was determined for an ionic strength of 0.06 at 20°C using the Güntelberg approximation [140].

(iii) The net convective mass flow (nmol s^{-1}) of each reaction species (X = H^+, CO_2, HCO_3^-, CO_3^{2-}, HA, A^-) from the upstream compartment into the compartment in consideration is

$$F_X = \rho \dot{Q}_b([X]_{upstream} - [X]), \tag{18}$$

where [X] and $[X]_{upstream}$ represent the species concentrations in the compartment in focus and in the upstream compartment. The factor ρ is the fraction of total hemolymph flow ($\dot{Q}_b$) that is fed into the outer hemolymph lacuna.

(iv) The rate (nmol s^{-1}) of transcuticular CO_2 diffusion, which depends on the difference in CO_2 partial pressure between the outer HL lacuna (P_{ho}) and the medium (P_m), is defined as

$$F_{Dt} = K \frac{A_{tr}\, dL/L}{\Delta x_{tr}} (P_{ho} - P_m). \tag{19}$$

Table 5: Parameter values of the CO_2 transport model.

Symbol	Value	Unit	Description
L	2.38	mm	Length of exchange coordinate
A_{ca}	7.57	mm^2	Exchange surface area of the inner carapace cuticle
A_{tr}	5.34	mm^2	Exchange surface area of the trunk cuticle
Δx_{ca}	0.001	mm	Thickness of the inner carapace cuticle
Δx_{tr}	0.002	mm	Thickness of the trunk cuticle
Q_b	0.022	$mm^3\ s^{-1}$	Perfusion rate
V_m	0.7	$mm^3\ s^{-1}$	Medium flow rate
v_b	0.168	$mm\ s^{-1}$	Hemolymph flow velocity, backward direction
v_f	0.149	$mm\ s^{-1}$	Hemolymph flow velocity, forward direction
v_m	1.8	$mm\ s^{-1}$	Medium flow velocity
M_{CO_2}	0.0071	$nmol\ s^{-1}$	Whole-animal CO_2 production rate
α_{CO_2}	0.3682	$nmol\ mm^{-3}\ kPa^{-1}$	Physical solubility of CO_2 in medium and hemolymph
K	2.10×10^{-6}	$nmol\ s^{-1}\ mm^{-1}\ kPa^{-1}$	Krogh's diffusion constant for CO_2 in chitin
K'_1	$10^{-6.325}$	M	Dissociation equilibrium constant of CO_2
K'_2	$10^{-10.47}$	M	Dissociation equilibrium constant of HCO_3^-
K'_A	$10^{-8.18}$	M	Dissociation equilibrium constant of the NB buffer
K'_w	10^{-14}	M	Dissociation equilibrium constant of water
k_1	0.022	s^{-1}	Rate constant for CO_2 hydration
k_2	10^{10}	$M^{-1}\ s^{-1}$	Rate constant for the protonation of CO_3^{2-}
k_3	5500	$M^{-1}\ s^{-1}$	Rate constant for the reaction of CO_2 with OH^-
k_{-3}	1.1×10^{-4}	s^{-1}	Rate constant for: $HCO_3^- \rightarrow CO_2 + OH^-$
k_4	10^{10}	$M^{-1}\ s^{-1}$	Rate constant for the protonation of the NB buffer
μ	1		Acceleration factor for CO_2/HCO_3^- interconversion
ρ	0.5		Fraction of $\dot{Q}_b$ entering the outer HL lacuna
ϕ	0.2		Fraction of CO_2 excreted into the outer HL lacuna
γ_H	0.797		Hydrogen activity coefficient

Table 5: Parameter values of the CO_2 transport model. *(Continued)*

C_A	3.6	nmol mm^{-3}	Concentration of the NB buffer in the hemolymph
P_{in}	0.035	kPa	Inspiratory CO_2 partial pressure
pH_{in}	8.0		pH of the inspired medium
$[HCO_3^-]_{in}$	0.6	nmol mm^{-3}	Bicarbonate concentration of the inspired medium

These parameter values were used to generate the profiles in acid-base variables shown in Figure 3D. The values for K and μ refer to the uncatalyzed case in the absence of a carbonic anhydrase in the hemolymph. The catalyzed case was derived from this parameter setting by two adjustments (μ = 10000, K = 1.30 × 10^{-6} nmol s^{-1} mm^{-1} kPa^{-1}). NB = non-bicarbonate.

K is Krogh's diffusion coefficient, whereas Δx_{tr} and $A_{tr}dL/L$ represents the thickness and surface area of the cuticular barrier at the hemolymph/medium interface.

The temporal changes in the concentration of all reaction partners for the specified compartment of volume V (= $\rho \dot{Q}_b\, dL/v_f$) are expressed as

$$d[H^+]/dt = R_1 - R_{-1} + R_2 - R_{-2} + R_3 - R_{-3} + R_4 - R_4 + F_{H^+}/V \quad (20)$$

$$d[CO_2]/dt = -R_1 + R_{-1} - R_3 + R_{-3} + (F_{CO_2} + \varphi F_{Ex} - F_{Dt})/V \quad (21)$$

$$d[HCO_3^-]/dt = R_1 - R_{-1} - R_2 + R_{-2} + R_3 - R_{-3} + F_{HCO_3^-}/V \quad (22)$$

$$d[CO_3^{2-}]/dt = R_2 - R_{-2} + F_{CO_3^{2-}}/V \quad (23)$$

$$d[HA]/dt = -R_4 + R_{-4} + F_{HA}/V \quad (24)$$

$$d[A^-]/dt = R_4 - R_{-4} + F_{A^-}/V \quad (25)$$

Parameter values (Table 5) related to geometry, convection and respiration were obtained from a reference model (R. Moenickes, O. Richter and R. Pirow, in preparation). All perfusion-related parameter values were set to 50% of the reference values to take the low heart rates of animals from the present study into account. The rate constants for the reaction of CO_2 with H_2O and OH^- at 20°C were obtained from [141]. The acceleration factor (μ) was set to 10000 [126], which is sufficiently large to attain an equilibrium in the $CO_2 + H_2O \leftrightarrow H^+ + HCO_3^-$ reaction. The protonation rate constant for the carbonate and the non-bicarbonate buffer was assumed to be of the magnitude of 10^{10} M^{-1} s^{-1} [111]. The dissociation equilibrium constants of all reaction species as well as the physical solubility of CO_2 were taken from the present study. An operational value for Krogh's diffusion constant (K) for CO_2 in chitin was chosen as such that the pH at the entrance of the inner hemolymph lacuna (Figure 3C) assumed a value of pH 8.334 under steady-state conditions. The cuticular barrier was assumed to be impermeable for all reaction species except CO_2, and the medium compartment lacked a non-bicarbonate buffer. The initial conditions for the hemolymph were pH 8.334 and 0.556 kPa P_{CO2}. The initial conditions of the medium compartment were set to the properties of the inspired medium (pH 8.06 and 0.035 kPa P_{CO2}). A number of N = 50 compartments was chosen per subdomain. Starting with the initial conditions, the model status was allowed to evolve until quasi steady-state conditions (relative concentration changes < 10^{-6}) were reached.

Statistics and Numerics

If not stated otherwise, data are expressed as means ± standard error, with N indicating the number of independent measurements. Differences in a physiological variable among the acclimation groups were checked using a one-way analysis on variance (ANOVA) or the Kruskal-Wallis test, depending on whether the data passed the normality test and the equal variance test. Statistical differences were considered as significant at $P < 0.05$. Multiple pairwise comparisons against the control (pH 7.8) group were performed using the Holm-Sidak test or Dunn's method, using an experimentwise significance level of 0.05. All statistical analyses were performed using SigmaStat (version 3.1; SPSS Inc.).

Numerical problems were solved in Matlab 7.0 (MathWorks, Inc.). The 'lsqnonlin' function (optimization toolbox) was used to fit the model in equation 1 to the P_{CO2}-pH data. The uncertainty in the calculation of P_{CO2}, given the pH and the calibration buffer curve, was determined by a nonlinear algorithm [142,143]. The 'rlowess' function (curve-fitting toolbox) was applied for the smoothing

of spectra. In-built functions for matrix operations (including that for the calculation of the Moore-Penrose pseudoinverse) were used to implement the reiterative least-squares spectral resolution [137] and the multicomponent analysis [139] (Additional file 4), whereas the 'fminsearch' function (optimization toolbox) provided the Nelder-Mead simplex algorithm [144]. The nonlinear system of ordinary differential equations (ODEs) was numerically solved using the 'ode15s' solver for stiff problems.

Annotations, sequence alignments and phylogenetic analysis

The *D. pulex* genome database was screened for carbonic anhydrase-like sequences by a keyword search in the automatically-created annotations and by a 'blastp alignment search' of the Dappu v1.1 gene builds (July, 2007) [117]. All gene models containing carbonic anhydrase-like sequences were manually curated and annotated (Table 4). The derived amino-acid sequences were classified using the conserved domain database (CDD) and search engine v2.13 [145,146]. Homolog sequences from other organisms were retrieved using the blastp algorithm [147]. All sequences were checked for the presence of N-terminal signal peptides using the SignalP V3.0 server [148-150]. Potential GPI-anchor sites were identified by GPI-SOM [151,152], the big-PI Predictor [153,154] and FragAnchor [155,156]. Multiple-sequence alignments were performed using the T-Coffee algorithm [157-159] and displayed with ESPript [160,161]. Phylogenetic trees were constructed using the neighbor-joining algorithm [162] and a bootstrap analysis with 1000 replicates. Trees were visualized using iTOL [163,164].

Abbreviations

A_{ca}: exchange surface area of the inner carapace cuticle; A_{tr}: exchange surface area of the trunk cuticle; C_A: concentration of the non-bicarbonate buffer; f_A: appendage beating rate; f_H: heart rate; F_{Dc}: rate of CO_2 diffusion across the inner carapace cuticle; F_{Dt}: rate of CO_2 diffusion across the trunk cuticle; F_{Ex}: CO_2 excretion rate; F_X: net convective mass flow (X = H^+, CO_2, HCO_3^-, CO_3^{2-}, HA, A^-); K: Krogh's diffusion constant for CO_2 in chitin; K'_1: first dissociation equilibrium constant of the carbonate system; K'_2: second dissociation equilibrium constants of the carbonate system; K'_A: dissociation equilibrium constant of the non-bicarbonate buffer; K'_a: dissociation equilibrium constant of cSNARF-1; K'_w: dissociation equilibrium constant of water; k_1, rate constant for CO_2 hydration; k_2: rate constant for the protonation of CO_3^{2-}; k_3, rate constant for the reaction of CO_2 with OH^-; k_{-3}: rate constant for the dissociation of HCO_3^- into CO_2 and OH^-; k_4: rate constant for the protonation of the non-bicarbonate buffer; L: length of the exchange coordinate; dL: compartment thickness; $\dot{M}_{CO_2}$: whole-animal CO_2 production rate; $\dot{M}_{O_2}$: volume-specific O_2 consumption rate; P_{CO2}: CO_2 partial pressure; P_{in}: inspiratory CO_2 partial pressure; P_{hi}: CO_2 partial pressure in the inner hemolymph lacuna; P_{ho}: CO_2 partial pressure in the outer hemolymph lacuna; P_m: CO_2 partial pressure in the medium; pH_{in}: pH values of the inspired medium; $\dot{Q}_b$: perfusion rate; R_Y: turnover rates (Y = 1, -1, 2, -2, 3, -3, 4, -4); SID: strong ion difference; V: compartment volume; $\dot{V}_m$: medium flow rate; v_b: hemolymph flow velocity in backward direction; v_f: hemolymph flow velocity in forward direction; v_m: medium flow velocity; α: fraction of acid; α_{CO2}: physical solubility of CO_2 in water and hemolymph; β_A: non-bicarbonate buffer value; β_B: bicarbonate buffer value; β_C: carbonate buffer value; β_T: total buffer value; ΔH^+: metabolic acid load; Δx_{ca}: thickness of the inner carapace cuticle; Δx_{tr}: thickness of the trunk cuticle; γ_H: H^+ activity coefficient; ρ: fraction of total hemolymph flow entering the outer hemolymph lacuna; ϕ: fraction of CO_2 excreted into the outer hemolymph lacuna; μ: acceleration factor for the interconversion between CO_2 and HCO_3^-.

Authors' contributions

AKW and RP conceived the study, carried out the methodical developments, and wrote the manuscript. AKW carried out the experiments. RP implemented the numerical tools, developed and implemented the CO_2 transport model, and annotated the carbonic anhydrase genes. Both authors read and approved the final manuscript.

Additional material

Additional file 1

***Multiple sequence alignment of α-carbonic anhydrases**. The α-CA sequences are divided into four groups according to similarity. Residues strictly conserved have a red background, residues well conserved within a group according to a Risler matrix [122] are indicated by red letters. Residues conserved between groups are boxed. Secondary structure elements of three human α-CAs are shown in blue on the top: helices with squiggles, beta strands with arrows, alpha and beta turns with TTT and TT letters. The numbering refers to HsCA2. Amino acid residues involved in zinc-binding and in the hydrogen-bonding network are indicated by red triangles. Yellow and orange backgrounds indicate mitochondrial targeting peptide or predicted signal peptides for secretory export. Pink and green backgrounds signify a transmembrane domain or potential glycosylphosphatidylinositol (GPI) anchor sites.* Daphnia pulex *sequences are indicated by red labels. Additionally included were related sequences from the blue crab* Callinectes sapidus *(Cs)*, Drosophila melanogaster *(Dm)*, Anopheles gambiae *(Ag)*, Caenorhabditis elegans *(Ce)*, *the sea urchin* Strongylocentrotus purpuratus *(Sp)*, *and* Homo sapiens *(Hs). Sequences were aligned using the T-Coffee algorithm [158] and displayed with ESPript [120,161]. Sequence references, protein data bank (PDB) codes and NCBI accession numbers:* Callinectes *[124]*, Drosophila *[119]*, Anopheles *[125]*, *HsCA2 (1CA2)*, *HsCA4 (1ZNC)*, *HsCA5A (NP_001730)*, *HsCA6 (P23280)*, *HsCA10 (AAH29865)*, *HsCA12 (1JCZ)*, *CeCAH2 (Q18932)*, *SpCA8 (XP_795365)*, *SpCAc (XP_782997)*, *SpCA-RP (XP_784796)*, *SpCA-GPI (XP_796525)*.
Click here for file
[http://www.biomedcentral.com/content/supplementary/1472-6793-9-9-S1.pdf]

Additional file 2

***Multiple sequence alignment of β-carbonic anhydrases**. Numbering and the secondary structure elements on the top refer to the β-CA from* Pisum sativum *(PsCAb) [121]. The other sequences are from* Daphnia pulex *(CAB)*, Drosophila melanogaster *(DmCG11967)*, Anopheles gambiae *(AgCAb)*, Caenorhabditis elegans *(CeCAb1)*, *sea urchin* Strongylocentrotus purpuratus *(SpCAb), and the sea anemone* Nematostella vectensis *(NvCAb). A column is framed in blue if more than 70% of its residues are similar according to physico-chemical properties. Similar residues are indicated by red letters; strictly conserved residues have a red background. Secondary structure elements are presented as follows: helices with squiggles, beta strands with arrows, alpha and beta turns with TTT and TT letters. Amino acid residues involved in zinc and substrate binding are indicated by red and blue triangles. Sequences were aligned using the T-Coffee algorithm [158] and displayed with ESPript [120,161]. Protein data bank (PDB) code and NCBI accession numbers: PsCAb (2EKJ), DmCG11967 (NP_649849), AgCAb (XP_563117), CeCAb1 (NP_741809), SpCAb (XP_786120), NvCAb (XP_001632619).*
Click here for file
[http://www.biomedcentral.com/content/supplementary/1472-6793-9-9-S2.pdf]

Additional file 3

***Determination of operational pK' values and correction for incomplete equilibration**. This supplement describes experimental determination of pK'_1 and pK'_2 from standard bicarbonate solutions (4, 8, and 16 mM $NaHCO_3$ plus 50 mM NaCl). It also outlines the analytical procedure for the correction of incomplete equilibration of bicarbonate and hemolymph samples at low CO_2 partial pressures.*
Click here for file
[http://www.biomedcentral.com/content/supplementary/1472-6793-9-9-S3.pdf]

Additional file 4

***Reiterative least-squares spectral resolution & multicomponent analysis**. This supplement describes the* reiterative least-squares spectral resolution, *which was employed for the determination of the pK'_a value and the acid/base spectra of cSNARF-1. It also outlines the* multicomponent analysis, *which was used to retrieve the* in vivo *pH from* in vivo *spectra of cSNARF.*
Click here for file
[http://www.biomedcentral.com/content/supplementary/1472-6793-9-9-S4.pdf]

Acknowledgements

We thank Dr. Stefan Hetz (Humboldt-University of Berlin) for his generous and lasting loan. The expert technical contributions of Ina Buchen and Olaf Pinkhaus (University of Münster) are also gratefully acknowledged.

The sequencing and portions of the analyses were performed at the DOE Joint Genome Institute under the auspices of the U.S. Department of Energy's Office of Science, Biological and Environmental Research Program, and by the University of California, Lawrence Livermore National Laboratory under Contract No. W-7405-Eng-48, Lawrence Berkeley National Laboratory under Contract No. DE-AC02-05CH11231, Los Alamos National Laboratory under Contract No. W-7405-ENG-36 and in collaboration with the Daphnia Genomics Consortium (DGC) http://daphnia.cgb.indiana.edu. Additional analyses were performed by wFleaBase, developed at the Genome Informatics Lab of Indiana University with support to Don Gilbert from the National Science Foundation and the National Institutes of Health. Coordination infrastructure for the DGC is provided by The Center for Genomics and Bioinformatics at Indiana University, which is supported in part by the METACyt Initiative of Indiana University, funded in part through a major grant from the Lilly Endowment, Inc. Our work benefits from, and contributes to the Daphnia Genomics Consortium.

References

1. Laudon H, Westling O, Bishop K: **Cause of pH decline in stream water during spring melt runoff in northern Sweden.** *Can J Fish Aquat Sci* 2000, **57(9):**1888-1900.
2. Lepori F, Ormerod SJ: **Effects of spring acid episodes on macroinvertebrates revealed by population data and in situ toxicity tests.** *Freshwat Biol* 2005, **50(9):**1568-1577.
3. Eppinger RG, Briggs PH, Dusel-Bacon C, Giles SA, Gough LP, Hammarstrom JM, Hubbard BE: **Environmental geochemistry at Red Mountain, an unmined volcanogenic massive sulphide deposit in the Bonnifield district, Alaska Range, east-central Alaska.** *Geochem: Explor Environ Anal* 2007, **7:**207-223.
4. Satake K, Oyagi A, Iwao Y: **Natural acidification of lakes and rivers in Japan: The ecosystem of Lake Usoriko (pH 3.4–3.8).** *Water Air Soil Pollut* 1995, **85(2):**511-516.

5. Ezoe Y, Lin CH, Noto M, Watanabe Y, Yoshimura K: **Evolution of water chemistry in natural acidic environments in Yangmingshan, Taiwan.** *J Environ Monit* 2002, **4(4):**533-540.
6. Hao JM, Tian HZ, Lu YQ: **Emission inventories of NO_x from commercial energy consumption in China, 1995–1998.** *Environ Sci Technol* 2002, **36(4):**552-560.
7. Moiseenko TI: **Effects of acidification on aquatic ecosystems.** *Russ J Ecol* 2005, **36(2):**93-102.
8. Kurvits T, Marta T: **Agricultural NH_3 and NO_x emissions in Canada.** *Environ Pollut* 1998, **102:**187-194.
9. Liu WX, Luan ZK, Tang HX: **Use of the sediment quality triad to assess metal contamination in freshwater superficial sediments from the Le An River, China.** *Water Air Soil Pollut* 1999, **113(1–4):**227-239.
10. Cappuyns V, Swennen R, Devivier A: **Dredged river sediments: Potential chemical time bombs? A case study.** *Water Air Soil Pollut* 2006, **171(1–4):**49-66.
11. Geller W, Klapper H, Salomons W: **Acidic mining lakes: Acid mine drainage, limnology and reclamation.** Berlin: Springer Verlag; 1998.
12. Deneke R: **Review of rotifers and crustaceans in highly acidic environments of pH values ≤ 3.** *Hydrobiologia* 2000, **433(1–3):**167-172.
13. Leivestad H, Hendrey G, Muniz IP, Snekvik E: **Effects of acid precipitation on freshwater organisms.** *Impact of acid precipitation on forest and freshwater ecosystems in Norway: Summary report on the research results from the phase I (1972–1975) of the SNSF-project. Oslo: SNSF Project FR6/76* 1976:86-111.
14. Brett MT: **Zooplankton communities and acidification processes (a review).** *Water Air Soil Pollut* 1989, **44(3–4):**387-414.
15. Brönmark C, Hansson L-A: **The biology of lakes and ponds.** Oxford: Oxford University Press; 1998.
16. Holt CA, Yan ND, Somers KM: **pH 6 as the threshold to use in critical load modeling for zooplankton community change with acidification in lakes of south-central Ontario: accounting for morphometry and geography.** *Can J Fish Aquat Sci* 2003, **60(2):**151-158.
17. Kurbatova SA: **[Response of microcosm zooplankton to acidification].** *Izv Akad Nauk Ser Biol* 2005:100-108.
18. Locke A: **Zooplankton responses to acidification: A review of laboratory bioassays.** *Water Air Soil Pollut* 1991, **60(1–2):**135-148.
19. Havens KE, Yan ND, Keller W: **Lake acidification: Effects on crustacean zooplankton populations.** *Environ Sci Technol* 1993, **27(8):**1621-1624.
20. Havas M, Likens GE: **Toxicity of aluminum and hydrogen ions to *Daphnia catawba*, *Holopedium gibberum*, *Chaoborus punctipennis*, and *Chironomus anthrocinus* from Mirror Lake, New Hampshire.** *Can J Zool* 1985, **63(5):**1114-1119.
21. Havens KE: **Aluminum binding to ion exchange sites in acid-sensitive versus acid-tolerant cladocerans.** *Environ Pollut* 1990, **64(2):**133-141.
22. Lawrence SG, Holoka MH: **Effects of low concentrations of cadmium on the crustacean zooplankton community of an artificially acidified lake.** *Can J Fish Aquat Sci* 1987, **44:**163-172.
23. Locke A, Sprules WG: **Effects of acidic pH and phytoplankton on survival and condition of *Bosmina longirostris* and *Daphnia pulex*.** *Hydrobiologia* 2000, **437(1–3):**187-196.
24. Wood CM: **The physiological problems of fish in acid waters.** In *Acid toxicity and aquatic animals* Edited by: Morris R, Taylor EW, Brown DJA, Brown JA. Cambridge: Cambridge University Press; 1989:125-152.
25. McMahon BR, Stuart SA: **The physiological problems of crayfish in acid waters.** In *Acid toxicity and aquatic animals* Edited by: Morris R, Taylor EW, Brown DJA, Brown JA. Cambridge: Cambridge University Press; 1989:171-200.
26. Mantel LH, Farmer LL: **Osmotic and ionic regulation.** In *The biology of crustacea: Internal anatomy and physiological regulation* Edited by: Mantel LH. New York: Academic Press; 1983:53-161.
27. Krogh A: **Osmotic regulation in aquatic animals.** Cambridge: Cambridge University Press; 1939.
28. Potts WTW, Parry G: **Osmotic and ionic regulation in animals.** Oxford: Pergamon Press; 1964.
29. Rasmussen AD, Andersen O: **Apparent water permeability as a physiological parameter in crustaceans.** *J Exp Biol* 1996, **199(12):**2555-2564.
30. Nilssen JP, Østdahl T, Potts WTW: **Species replacements in acidified lakes: Physiology, predation or competition.** *Rep Inst Freshw Res Drottningholm* 1984, **61:**148-153.
31. Vangenechten JHD, Witters H, Vanderborght OLJ: **Laboratory studies on invertebrate survival and physiology in acid waters.** In *Acid toxicity and aquatic animals* Edited by: Morris R, Taylor EW, Brown DJA, Brown JA. Cambridge: Cambridge University Press; 1989:153-169.
32. Havas M, Advokaat E: **Can sodium regulation be used to predict the relative acid-sensitivity of various life-stages and different species of aquatic fauna?** *Water Air Soil Pollut* 1995, **85(2):**865-870.
33. Potts WTW, Fryer G: **The effects of pH and salt content on sodium balance in *Daphnia magna* and *Acantholeberis curvirostris* (Crustacea: Cladocera).** *J Comp Physiol* 1979, **129(4):**289-294.
34. Havas M, Hutchinson TC, Likens GE: **Effect of low pH on sodium regulation in two species of *Daphnia*.** *Can J Zool* 1984, **62(10):**1965-1970.
35. Glover CN, Wood CA: **Physiological characterisation of a pH- and calcium-dependent sodium uptake mechanism in the freshwater crustacean, *Daphnia magna*.** *J Exp Biol* 2005, **208(5):**951-959.
36. Pirow R, Wollinger F, Paul RJ: **The sites of respiratory gas exchange in the planktonic crustacean *Daphnia magna*: An in vivo study employing blood haemoglobin as an internal oxygen probe.** *J Exp Biol* 1999, **202(22):**3089-3099.
37. Péqueux A: **Osmotic Regulation in Crustaceans.** *J Crustacean Biol* 1995, **15(1):**1-60.
38. Zetino AM, Kirschner LB, Harvey M: **On the mechanism of sodium-proton exchange in crayfish.** *Comp Biochem Physiol A Mol Integr Physiol* 2001, **128(4):**863-872.
39. Evans DH, Piermarini PM, Choe KP: **The multifunctional fish gill: Dominant site of gas exchange, osmoregulation, acid-base regulation, and excretion of nitrogenous waste.** *Physiol Rev* 2005, **85(1):**97-177.
40. Kirschner LB: **The mechanism of sodium chloride uptake in hyperregulating aquatic animals.** *J Exp Biol* 2004, **207(9):**1439-1452.
41. Whiteley NM: **Acid-base regulation in crustaceans: the role of bicarbonate ions.** In *Regulation of acid-base status in animals and plants* Edited by: Egginton S, Taylor EW, Raven JA. Cambridge: Cambridge University Press; 1999.
42. Poynton HC, Varshavsky JR, Chang B, Cavigiolio G, Chan S, Holman PS, Loguinov AV, Bauer DJ, Komachi K, Theil EC, *et al.*: ***Daphnia magna* ecotoxicogenomics provides mechanistic insights into metal toxicity.** *Environ Sci Technol* 2007, **41(3):**1044-1050.
43. Shaw JR, Colbourne JK, Davey JC, Glaholt SP, Hampton TH, Chen CY, Folt CL, Hamilton JW: **Gene response profiles for *Daphnia pulex* exposed to the environmental stressor cadmium reveals novel crustacean metallothioneins.** *BMC Genomics* 2007, **8:**477.
44. Soetaert A, Vandenbrouck T, Ven K van der, Maras M, van Remortel P, Blust R, de Coen WM: **Molecular responses during cadmium-induced stress in *Daphnia magna*: Integration of differential gene expression with higher-level effects.** *Aquat Toxicol* 2007, **83(3):**212-222.
45. Connon R, Hooper HL, Sibly RM, Lim FL, Heckmann LH, Moore DJ, Watanabe H, Soetaert A, Cook K, Maund SJ, *et al.*: **Linking molecular and population stress responses in *Daphnia magna* exposed to cadmium.** *Environ Sci Technol* 2008, **42(6):**2181-2188.
46. Heckmann LH, Sibly RM, Connon R, Hooper HL, Hutchinson TH, Maund SJ, Hill CJ, Bouetard A, Callaghan A: **Systems biology meets stress ecology: linking molecular and organismal stress responses in *Daphnia magna*.** *Genome Biol* 2008, **9(2):**R40.
47. Eads BD, Andrews J, Colbourne JK: **Ecological genomics in *Daphnia*: stress responses and environmental sex determination.** *Heredity* 2008, **100(2):**184-190.
48. Pane EF, McGeer JC, Wood CM: **Effects of chronic waterborne nickel exposure on two successive generations of *Daphnia magna*.** *Environ Toxicol Chem* 2004, **23(4):**1051-1056.
49. Pane EF, Smith C, McGeer JC, Wood CM: **Mechanisms of acute and chronic waterborne nickel toxicity in the freshwater cladoceran, *Daphnia magna*.** *Environ Sci Technol* 2003, **37(19):**4382-4389.

50. Cameron JN: **Effects of hypercapnia on blood acid-base status, NaCl fluxes, and trans-gill potential in freshwater blue crabs, *Callinectes sapidus*.** *Journal of Comparative Physiology* 1978, **123(2):**137-141.
51. Cameron JN: **Acid-base responses to changes in CO_2 in two pacific crabs: The coconut crab, *Birgus latro*, and a mangrove crab, *Cardisoma carnifex*.** *Journal of Experimental Zoology* 1981, **218(1):**65-73.
52. Chen JC, Chen JS: **Acid-base balance, ammonia and lactate levels in the haemolymph of *Penaeus japonicus* during aerial exposure.** *Comp Biochem Physiol A Mol Integr Physiol* 1998, **121(3):**257-262.
53. deFur PL, Wilkes PRH, McMahon BR: **Non-equilibrium acid-base status in *C. productus*: Role of exoskeletal carbonate buffers.** *Respir Physiol* 1980, **42(3):**247-261.
54. Greenaway P, Bonaventura J, Taylor HH: **Aquatic gas exchange in the australian freshwater/land crabs of the genus *Holthuisana*.** *J Exp Biol* 1983, **103(Mar):**225-236.
55. Innes AJ, Forster ME, Jones MB, Marsden ID, Taylor HH: **Bimodal respiration, water balance and acid-base regulation in a high-shore crab, *Cyclograpsus lavauxi* H. Milne Edwards.** *Journal of Experimental Marine Biology and Ecology* 1986, **100(1–3):**127-145.
56. McMahon B, Sinclair F, Hassall CD, Defur PL, Wilkes PRH: **Ventilation and control of acid-base status during temperature acclimation in the crab, *Cancer magister*.** *Journal of Comparative Physiology* 1978, **128(2):**109-116.
57. McMahon BR, Butler PJ, Taylor EW: **Acid base changes during recovery from disturbance and during long term hypoxic exposure in the lobster *Homarus vulgaris*.** *Journal of Experimental Zoology* 1978, **205(3):**361-370.
58. Morris S, Edwards T: **Circulatory, acid-base and respiratory responses of the purple shore crab *Leptograpsus variegatus* to immersion.** *Journal of Experimental Marine Biology and Ecology* 1996, **196(1–2):**189-211.
59. Morris S, Taylor AC, Bridges CR, Grieshaber MK: **Respiratory properties of the hemolymph of the intertidal prawn *Palaemon elegans* (Rathke).** *J Exp Zool* 1985, **233(2):**175-186.
60. Sartoris FJ: **Ökophysiologische Untersuchungen zur Säuresensitivität der Bachflohkrebse *Gammarus pulex* (L.) und *Gammarus fossarum* (Koch).** [PhD thesis, University of Düsseldorf]. Aachen: Verlag Shaker; 1992.
61. Sinha NP, Dejours P: **Ventilation and blood acid-base balance of the crayfish as functions of water oxygenation (40–1500 torr).** *Comp Biochem Physiol A Physiol* 1980, **65(4):**427-432.
62. Spicer JI, Raffo A, Widdicombe S: **Influence of CO_2-related seawater acidification on extracellular acid-base balance in the velvet swimming crab *Necora puber*.** *Mar Biol* 2007, **151(3):**1117-1125.
63. Taylor AC, Davies PS: **Aquatic respiration in the land crab, *Gecarcinus lateralis* (Fréminville).** *Comp Biochem Physiol A Physiol* 1982, **72(4):**683-688.
64. Taylor EW, Wheatly MG: **The effect of long-term aerial exposure on heart rate, ventilation, respiratory gas exchange and acid-base status in the crayfish *Austropotamobius pallipes*.** *J Exp Biol* 1981, **92(Jun):**109-124.
65. Taylor EW, Whiteley NM: **Oxygen transport and acid-base balance in the haemolymph of the lobster, *Homarus gammarus*, during aerial exposure and resubmersion.** *J Exp Biol* 1989, **144:**417-436.
66. Truchot JP: **Blood acid-base changes during experimental emersion and reimmersion of the intertidal crab *Carcinus maenas* (L.).** *Respir Physiol* 1975, **23(3):**351-360.
67. Varley DG, Greenaway P: **The effect of emersion on hemolymph acid-base balance and oxygen levels in *Scylla serrata* Forskal (Brachyura: Portunidae).** *J Exp Mar Biol Ecol* 1992, **163(1):**1-12.
68. Weber RE, Hagerman L: **Oxygen and carbon dioxide transporting qualities of hemocyanin in the hemolymph of a natant decapod *Palaemon adspersus*.** *Journal of Comparative Physiology* 1981, **145(1):**21-27.
69. Wheatly MG, Mcmahon BR: **Responses to hypersaline exposure in the euryhaline crayfish *Pacifastacus leniusculus*. I. The interaction between ionic and acid-base regulation.** *J Exp Biol* 1982, **99(Aug):**425-445.
70. Wilkes PRH, McMahon BR: **Effect of maintained hypoxic exposure on the crayfish *Orconectes rusticus*. I. Ventilatory, acid-base and cardiovascular adjustments.** *J Exp Biol* 1982, **98(Jun):**119-137.
71. Pirow R, Buchen I: **The dichotomous oxyregulatory behaviour of the planktonic crustacean *Daphnia magna*.** *J Exp Biol* 2004, **207(4):**683-696.
72. Schmidt-Nielsen K: **Scaling: Why is animal size so important?** Cambridge: Cambridge University Press; 1984.
73. Pirow R, Bäumer C, Paul RJ: **Benefits of haemoglobin in the cladoceran crustacean *Daphnia magna*.** *J Exp Biol* 2001, **204(20):**3425-3441.
74. Seidl MD, Paul RJ, Pirow R: **Effects of hypoxia acclimation on morpho-physiological traits over three generations of *Daphnia magna*.** *J Exp Biol* 2005, **208(11):**2165-2175.
75. Seidl MD, Pirow R, Paul RJ: **Acclimation of the microcrustacean *Daphnia magna* to warm temperatures is dependent on haemoglobin expression.** *J Therm Biol* 2005, **30(7):**532-544.
76. Pirow R, Baumer C, Paul RJ: **Crater landscape: two-dimensional oxygen gradients in the circulatory system of the microcrustacean *Daphnia magna*.** *J Exp Biol* 2004, **207(25):**4393-4405.
77. Morgan DO, McMahon BR: **Acid tolerance and effects of sublethal acid exposure on iono-regulation and acid-base status in two crayfish *Procambarus clarki* and *Orconectes rusticus*.** *J Exp Biol* 1982, **97(Apr):**241-252.
78. Wood CM, Rogano MS: **Physiological responses to acid stress in crayfish (*Orconectes*): Hemolymph ions, acid-base status, and exchanges with the environment.** *Can J Fish Aquat Sci* 1986, **43(5):**1017-1026.
79. Jensen FB, Malte H: **Acid-base and electrolyte regulation, and hemolymph gas transport in crayfish, *Astacus astacus*, exposed to soft, acid water with and without aluminum.** *J Comp Physiol B* 1990, **160(5):**483-490.
80. McMahon BR, Morgan DO: **Acid toxicity and physiological responses to sub-lethal acid exposure in crayfish.** In *Freshwater crayfish V: Papers from the fifth international symposium on freshwater crayfish* Edited by: Goldman CR. Westport: AVI Publishing; 1983:71-85.
81. Malley DF: **Decreased survival and calcium uptake by the crayfish *Orconectes virilis* in low pH.** *Can J Fish Aquat Sci* 1980, **37(3):**364-372.
82. France RL: **Response of the crayfish *Orconectes virilis* to experimental acidification of a lake with special reference to the importance of calcium.** In *Freshwater crayfish V: Papers from the fifth international symposium on freshwater crayfish* Edited by: Goldman CR. Westport: AVI Publishing; 1983:98-111.
83. Zanotto FP, Wheatly MG: **The effect of ambient pH on electrolyte regulation during the postmolt period in freshwater crayfish *Procambarus clarkii*.** *J Exp Biol* 1993, **178:**1-19.
84. Kring RL, O'Brien WJ: **Effect of varying oxygen concentrations on the filtering rate of *Daphnia pulex*.** *Ecology* 1976, **57(4):**808-814.
85. Glazier DS: **Separating the respiration rates of embryos and brooding females of *Daphnia magna*: Implications for the cost of brooding and the allometry of metabolic rate.** *Limnol Oceanogr* 1991, **36(2):**354-362.
86. Sterba G: **Zytologische Untersuchungen an grosskernigen Fettzellen von *Daphnia pulex* unter besonderer Berücksichtigung des Mitochondrien-Formwechsels.** *Z Zellforsch Mikrosk Anat* 1956, **44(5):**456-487.
87. Tessier AJ, Goulden CE: **Estimating food limitation in cladoceran populations.** *Limnol Oceanogr* 1982, **27(4):**707-717.
88. Bodar CWM, van Donselaar EG, Herwig HJ: **Cytopathological investigations of digestive tract and storage cells in *Daphnia magna* exposed to cadmium and tributyltin.** *Aquat Toxicol* 1990, **17(4):**325-338.
89. Green J: **Carotenoids in *Daphnia*.** *Proc R Soc Lond Ser B Biol Sci* 1957, **147(928):**392-401.
90. Goldmann T, Becher B, Wiedorn KH, Pirow R, Deutschbein ME, Vollmer E, Paul RJ: **Epipodite and fat cells as sites of hemoglobin synthesis in the branchiopod crustacean *Daphnia magna*.** *Histochem Cell Biol* 1999, **112(5):**335-339.
91. Zaffagnini F, Zeni C: **Considerations on some cytological and ultrastructural observations on fat cells of *Daphnia* (Crustacea, Cladocera).** *Boll Zool* 1986, **53(1):**33-39.
92. Olmstead AW, Leblanc GA: **Juvenoid hormone methyl farnesoate is a sex determinant in the crustacean *Daphnia magna*.** *J Exp Zool* 2002, **293(7):**736-739.

93. Rider CV, Gorr TA, Olmstead AW, Wasilak BA, Leblanc GA: **Stress signaling: coregulation of hemoglobin and male sex determination through a terpenoid signaling pathway in a crustacean.** *J Exp Biol* 2005, **208(1):**15-23.
94. Seymour R, Cowgill UM, Klecka GM, Gersich FM, Mayes MA: **Occurrence of *Aphanomyces daphniae* infection in laboratory cultures of *Daphnia magna*.** *J Invertebr Pathol* 1984, **43(1):**109-113.
95. Stazi AV, Mantovani A, Fuglieni F, Didelupis GLD: **Observations on fungal infection of the ovary of laboratory-cultured *Daphnia magna*.** *Bull Environ Contam Toxicol* 1994, **53(5):**699-703.
96. France RL, Graham L: **Increased microsporidian parasitism of the crayfish *Orconectes virilis* in an experimentally acidified lake.** *Water Air Soil Pollut* 1985, **26(2):**129-136.
97. Ebert D: **Ecology, epidemiology, and evolution of parasitism in *Daphnia* [Internet].** Bethesda (MD): National Library of Medicine (US), National Center for Biotechnology Information; 2005.
98. Havas M, Likens GE: **Changes in ^{22}Na influx and outflux in *Daphnia magna* (Straus) as a function of elevated Al concentrations in soft water at low pH.** *Proc Natl Acad Sci USA* 1985, **82(21):**7345-7349.
99. Havas M, Hutchinson TC: **Effect of low pH on the chemical composition of aquatic invertebrates from tundra ponds at the Smoking Hills, N.W.T., Canada.** *Can J Zool* 1983, **61(1):**241-249.
100. Stobbart RH, Keating J, Earl R: **A study of sodium uptake by the water flea *Daphnia magna*.** *Comp Biochem Physiol A Physiol* 1977, **58(3):**299-309.
101. Bianchini A, Wood CM: **Physiological effects of chronic silver exposure in *Daphnia magna*.** *Comp Biochem Physiol C Toxicol Pharmacol* 2002, **133(1–2):**137-145.
102. Kobayashi M: **Estimation of the haemolymph volume in *Daphnia magna* by haemoglobin determination.** *Comp Biochem Physiol A Physiol* 1983, **76(4):**803-805.
103. Holm-Jensen I: **Osmotic regulation in *Daphnia magna* under physiological conditions and in the presence of heavy metals.** *K Dan Vidensk Selsk Biol Medd* 1948, **20:**1-64.
104. Roughton FJW: **Some recent work on the chemistry of carbon dioxide transport by blood.** *The Harvey lectures* 1943, **29:**96-142.
105. Gray BA: **The rate of approach to equilibrium in uncatalyzed CO_2 hydration reactions: The theoretical effect of buffering capacity.** *Respir Physiol* 1971, **11(2):**223-234.
106. Aldridge JB, Cameron JN: **CO_2 exchange in the blue crab, *Callinectes sapidus* (Rathbun).** *J Exp Zool* 1979, **207(2):**321-328.
107. Burnett LE, Woodson PBJ, Rietow MG, Vilicich VC: **Crab gill intraepithelial carbonic anhydrase plays a major role in haemolymph CO_2 and chloride ion regulation.** *J Exp Biol* 1981, **92(Jun):**243-254.
108. Henry RP, Cameron JN: **The distribution and partial characterization of carbonic anhydrase in selected aquatic and terrestrial decapod crustaceans.** *J Exp Zool* 1982, **221(3):**309-321.
109. Cameron JN, Heisler N: **Acid-base equilibria in invertebrates.** In *Acid-Base Regulation in Animals* Amsterdam: Elsevier; 1986:357-394.
110. Keen RE, Spain JD: **Computer simulation in biology: a BASIC introduction.** New York: Wiley-Liss; 1991.
111. Swietach P, Leem CH, Spitzer KW, Vaughan-Jones RD: **Experimental generation and computational modeling of intracellular pH gradients in cardiac myocytes.** *Biophys J* 2005, **88(4):**3018-3037.
112. Pirow R: **The contribution of hemoglobin to oxygen transport in the microcrustacean *Daphnia magna* – A conceptual approach.** *Adv Exp Med Biol* 2003, **510:**101-107.
113. Krogh A: **The rate of diffusion of gases through animal tissue, with some remarks on the coefficient of invasion.** *J Physiol (Lond)* 1919, **52:**391-408.
114. Dejours P: **Principles of comparative respiratory physiology.** Amsterdam: Elsevier/North-Holland Biomedical Press; 1981.
115. Martin JW: **Concise encyclopedia of the structure of animals.** Amsterdam: Elsevier; 2006.
116. wFleaBase: ***FlyBase: Daphnia* water flea genome database.** [http://wFleaBase.org].
117. JGI: **Joint Genome Institute.** [http://www.jgi.doe.gov/Daphnia].
118. Hewett-Emmett D, Tashian RE: **Functional diversity, conservation, and convergence in the evolution of the α-, β-, and γ-carbonic anhydrase gene families.** *Mol Phylogenet Evol* 1996, **5(1):**50-77.
119. FlyBase: **A database of *Drosophila* genes & genomes.** [http://flybase.org].
120. Gouet P, Robert X, Courcelle E: **ESPript/ENDscript: Extracting and rendering sequence and 3D information from atomic structures of proteins.** *Nucleic Acids Res* 2003, **31(13):**3320-3323.
121. Kimber MS, Pai EF: **The active site architecture of *Pisum sativum* β-carbonic anhydrase is a mirror image of that of α-carbonic anhydrases.** *EMBO J* 2000, **19(7):**1407-1418.
122. Risler JL, Delorme MO, Delacroix H, Henaut A: **Amino acid substitutions in structurally related proteins – a pattern recognition approach: Determination of a new and efficient scoring matrix.** *Journal of Molecular Biology* 1988, **204(4):**1019-1029.
123. Castro Nda S, Maia ZA, Pereira M, Soares CM: **Screening for glycosylphosphatidylinositol-anchored proteins in the *Paracoccidioides brasiliensis* transcriptome.** *Genet Mol Res* 2005, **4(2):**326-345.
124. Serrano L, Halanych KM, Henry RP: **Salinity-stimulated changes in expression and activity of two carbonic anhydrase isoforms in the blue crab *Callinectes sapidus*.** *J Exp Biol* 2007, **210(13):**2320-2332.
125. Smith KE, VanEkeris LA, Linser PJ: **Cloning and characterization of AgCA9, a novel α-carbonic anhydrase from *Anopheles gambiae* Giles *sensu stricto* (Diptera: Culicidae) larvae.** *J Exp Biol* 2007, **210(22):**3919-3930.
126. Geers C, Gros G: **Carbon dioxide transport and carbonic anhydrase in blood and muscle.** *Physiol Rev* 2000, **80(2):**681-715.
127. Gilmour KM: **The disequilibrium pH: A tool for the localization of carbonic anhydrase.** *Comp Biochem Physiol A Mol Integr Physiol* 1998, **119(1):**243-254.
128. Elendt BP, Bias WR: **Trace nutrient deficiency in *Daphnia magna* cultured in standard medium for toxicity testing. Effects of the optimization of culture conditions on life history parameters of *D. magna*.** *Water Res* 1990, **24(9):**1157-1167.
129. Walton WE, Compton SM, Allan JD, Daniels RE: **The effect of acid stress on survivorship and eeproduction of *Daphnia pulex* (Crustacea, Cladocera).** *Can J Zool* 1982, **60(4):**573-579.
130. Paul RJ, Colmorgen M, Hüller S, Tyroller F, Zinkler D: **Circulation and respiratory control in millimetre-sized animals (*Daphnia magna*, *Folsomia candida*) studied by optical methods.** *J Comp Physiol B Biochem Syst Environ Physiol* 1997, **167(6):**399-408.
131. Truchot JP: **Comparative aspects of extracellular acid-base balance.** Berlin: Springer-Verlag; 1987.
132. Stewart PA: **Independent and dependent variables of acid-base control.** *Respir Physiol* 1978, **33(1):**9-26.
133. Duan Z, Sun R: **An improved model calculating CO_2 solubility in pure water and aqueous NaCl solutions from 273 to 533 K and from 0 to 2000 bar.** *Chem Geol* 2003, **193(3–4):**257-271.
134. Duan Z, Sun R, Zhu C, Chou I-M: **An improved model for the calculation of CO_2 solubility in aqueous solutions containing Na^+, K^+, Ca^{2+}, Mg^{2+}, Cl^-, and SO_4^{2-}.** *Mar Chem* 2006, **98(2–4):**131-139.
135. Burton RF: **The roles of buffers in body fluids: mathematical analysis.** *Respir Physiol* 1973, **18(1):**34-42.
136. Heisler N: **Buffering and transmembrane ion transfer processes.** In *Acid-base regulation in animals* Edited by: Heisler N. Amsterdam: Elsevier; 1986:3-47.
137. Frans SD, Harris JM: **Reiterative least-squares spectral resolution of organic/acid base mixtures.** *Anal Chem* 1984, **56(3):**466-470.
138. Green J: **Growth, size and reproduction in *Daphnia* (Crustacea: Cladocera).** *Proc Zool Soc Lond* 1956, **126:**173-204.
139. Vandegriff KD, Shrager RI: **Hemoglobin-oxygen equilibrium binding: Rapid-scanning spectrophotometry and singular value decomposition.** In *Methods in Enzymology, Hemoglobins, Part C: Biophysical methods Volume 232*. Edited by: Everse J, Vandengriff KD, Winslow RM. New York: Academic Press; 1994:460-485.
140. Stumm W, Morgan JJ: **Aquatic Chemistry.** New York: John Wiley & Sons, Inc; 1995.
141. Portielje R, Lijklema L: **Carbon dioxide fluxes across the air-water interface and its impact on carbon availability in aquatic systems.** *Limnol Oceanogr* 1995, **40(4):**690-699.
142. Tellinghuisen J: **A simple, all-purpose nonlinear algorithm for univariate calibration.** *Analyst* 2000, **125(6):**1045-1048.
143. Tellinghuisen J: **Simple algorithms for nonlinear calibration by the classical and standard additions methods.** *Analyst* 2005, **130(3):**370-378.

144. Press WH, Teukolsky SA, Vetterling WT, Flannery BP: **Numerical recipes in C: The art of scientific computing.** 2nd edition. Cambridge: Cambridge University Press; 1992.
145. CDD: **Conserved Domain Database.** [http://www.ncbi.nlm.nih.gov/Structure/cdd/cdd.shtml].
146. Marchler-Bauer A, Anderson JB, Derbyshire MK, DeWeese-Scott C, Gonzales NR, Gwadz M, Hao LN, He SQ, Hurwitz DI, Jackson JD, *et al.*: **CDD: a conserved domain database for interactive domain family analysis.** *Nucleic Acids Res* 2007, **35:**D237-D240.
147. **NCBI blastp** [http://www.ncbi.nlm.nih.gov/blast/Blast.cgi]
148. **SignalP 3.0 server** [http://www.cbs.dtu.dk/services/SignalP/]
149. Bendtsen JD, Nielsen H, von Heijne G, Brunak S: **Improved prediction of signal peptides: SignalP 3.0.** *J Mol Biol* 2004, **340(4):**783-795.
150. Emanuelsson O, Brunak S, von Heijne G, Nielsen H: **Locating proteins in the cell using TargetP, SignalP and related tools.** *Nature Protocols* 2007, **2(4):**953-971.
151. GPI-SOM: **Identification of GPI-anchor signals.** [http://gpi.unibe.ch].
152. Fankhauser N, Maser P: **Identification of GPI anchor attachment signals by a Kohonen self-organizing map.** *Bioinformatics* 2005, **21(9):**1846-1852.
153. big-PI Predictor: **GPI modification site prediction.** [http://mendel.imp.ac.at/sat/gpi/gpi_server.html].
154. Eisenhaber B, Bork P, Eisenhaber F: **Prediction of potential GPI-modification sites in proprotein sequences.** *J Mol Biol* 1999, **292(3):**741-758.
155. **FragAnchor: GPI-anchored protein prediction** [http://navet.ics.hawaii.edu/~fraganchor/NNHMM/NNHMM.html]
156. Poisson G, Chauve C, Chen X, Bergeron A: **FragAnchor: A large-scale predictor of glycosylphosphatidylinositol anchors in eukaryote protein sequences by qualitative scoring.** *Geno Prot Bioinfo* 2007, **5(2):**121-130.
157. **T-Coffee: multiple sequence alignment tool** [http://www.tcoffee.org]
158. Notredame C, Higgins DG, Heringa J: **T-Coffee: A novel method for fast and accurate multiple sequence alignment.** *J Mol Biol* 2000, **302(1):**205-217.
159. Poirot O, O'Toole E, Notredame C: **Tcoffee@igs: a web server for computing, evaluating and combining multiple sequence alignments.** *Nucleic Acids Res* 2003, **31(13):**3503-3506.
160. **ESPript: PostScript output from aligned sequences** [http://espript.ibcp.fr/ESPript/cgi-bin/ESPript.cgi]
161. Gouet P, Courcelle E, Stuart DI, Metoz F: **Analysis of multiple sequence alignments in PostScript.** *Bioinformatics* 1999, **15(4):**305-308.
162. Saitou N, Nei M: **The neighbor-joining method: A new method for reconstructing phylogenetic trees.** *Mol Biol Evol* 1987, **4(4):**406-425.
163. iTOL: **Interactive Tree Of Life.** [http://itol.embl.de].
164. Letunic I, Bork P: **Interactive Tree Of Life (iTOL): an online tool for phylogenetic tree display and annotation.** *Bioinformatics* 2007, **23(1):**127-128.